CHALMERS

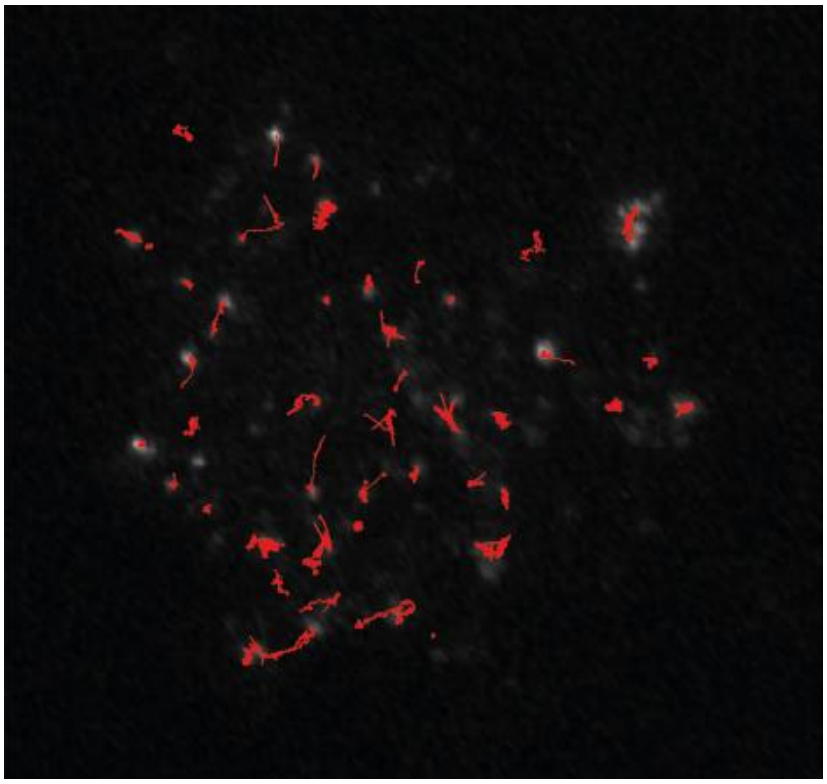

Towards an Assay for Liposome-based Vaccine Uptake by Dendritic Cells

Using TIRF Microscopy and Single Particle Tracking

Master of Science Thesis in the Master's Degree Programme Biotechnology

KARIN NORLING

Department of Applied Physics
Division of Biological Physics
CHALMERS UNIVERSITY OF TECHNOLOGY
Gothenburg, Sweden, 2014

Towards an Assay for Liposome-based Vaccine Uptake by Dendritic Cells

Using TIRF Microscopy and Single Particle Tracking

KARIN NORLING

Department of Applied Physics

Chalmers University of Technology

Gothenburg, Sweden 2014

Towards an Assay for Liposome-based Vaccine Uptake by Dendritic Cells

Using TIRF Microscopy and Single Particle Tracking

KARIN NORLING

Department of Applied Physics

Chalmers University of Technology

SE-412 96 Gothenburg

Sweden

Telephone: + 46 (0)31-772 1000

Cover: Trajectories (red) of liposomes (white) functionalized with the CTA1-3M2e-DD-construct, attached to a dendritic cell. Imaging was performed with TIRF microscopy and trajectories were obtained with single particle tracking.

Printed at Chalmers Reproservice

Gothenburg, Sweden 2014

Towards an Assay for Liposome-based Vaccine Uptake by Dendritic Cells
Using TIRF Microscopy and Single Particle Tracking

KARIN NORLING
Department of Applied Physics
Chalmers University of Technology

ABSTRACT

There are rising concerns that an inevitable Influenza A outbreak of pandemic proportions will spread at a previously unmatched rate due to the nature of our modern travel habits. It is therefore becoming increasingly urgent to develop effective, safe and easily administered vaccines suitable for use in a pandemic situation. Recently, increasing focus has been laid on the development of nanocarriers for vaccination compounds with liposomes being promising carrier candidates. Liposomes are almost endlessly customizable which makes finding the optimal formulation a difficult task. Furthermore, little is currently known about how the rate and mode of uptake of a vaccine formulation by immune cells correlates to the induced immunity, and improved knowledge of this process would allow rationalization of the development of vaccine formulations. The aim of this master's thesis was therefore the development of an assay for the characterization and quantification of uptake of liposomes functionalized with an influenza vaccine compound candidate, by dendritic cells. To this end, total internal reflection fluorescence (TIRF) microscopy, epifluorescence microscopy and single particle tracking was applied and different assay approaches were evaluated. TIRF microscopy was used to probe the movement of cell-bound, fluorescently labelled liposomes at the basal membrane. The results revealed that the movement of individual liposomes was largely confined, or possibly directed. However, no uptake events by membrane fusion or by endocytosis could be clearly identified in these experiments. Epifluorescence microscopy was used in an attempt to quantify the overall liposome uptake by recording the change over time in the number of cell-bound liposomes. However, no decrease in the number of attached liposomes could be established. The work performed in this master's thesis represents the first step towards the establishment of an assay for the study of uptake of functionalized liposomes by dendritic cells and gives useful practical insight into the possibilities and pitfalls of the set-up.

Keywords: total internal reflection fluorescence microscopy, TIRF microscopy, single particle tracking, cellular uptake, dendritic cells, liposomes, CTA1-3M2e-DD, mucosal vaccine.

Acknowledgements

Marta Bally, my supervisor and examiner, thank you for this opportunity and for your never-ending support and enthusiasm in all things, big and small. Your guidance has been truly invaluable.

Dubravka Grdic Eliasson, Samer Shkoukani, and Nils Lycke, the collaborators at Sahlgrenska, thank you for providing the cells as well as priceless advice and practical help regarding their care.

Patric Wallin and Julie Gold, thanks for taking an interest in the project, for your help and advice and for letting me use the cell lab.

Stephan Block, thank you for your invaluable expertise on single particle tracking and for providing emergency MATLAB support.

Sabina Burazerovic, thank you for your expertise and assistance in liposome fabrication and functionalization.

The Biological Physics group, you are such a genuinely lovely group of people and I want to thank you all for your generosity when it comes to answering questions, sharing ideas, encouragement and good times.

The five years leading up to this thesis have been challenging at times (most of the time) and would have been impossible without the support and encouragement from those closest to me. I would like to thank my family and the wonderful friends I have had the fortune of sharing this time with. Last but not least, Joakim, thank you for your kindness, patience and love these past years. Let's hope our next chapter involves a dishwasher.

TABLE OF CONTENTS

1 INTRODUCTION

Nanoparticles, and in particular liposomes, have attracted considerable attention as carriers in drug delivery and vaccination, as they provide a way to change the pharmacokinetics and biodistribution of compounds while providing possibilities to target specific tissues or cell types [1, 2]. Liposomes, nano- or micro-sized hollow spheres made of bilayered phospholipid membranes, were discovered by Bangham *et al*. in 1965 [3] and were first used as drug carriers by Gregoriadis *et al*. in 1974 [4]. The interest for liposomes in this context has since then steadily increased. The great advantage of liposomes is their versatility. They can be loaded with vastly different types of compounds while their physicochemical properties are easily customized, for example to enhance their inherent immunological adjuvanticity [5, 6]. Furthermore, they are biocompatible and biodegradable when made with lipids found in the native cell membrane [7], making them good candidates for use as vaccine carriers.

The supply of effective, safe and easily administered vaccines is becoming exceedingly important as our modern travel habits make us vulnerable to rapid regional and global spread of disease [8, 9]. A disease that regularly causes both minor and major epidemics is influenza, a highly contagious respiratory disease caused by a virus of the *Orthomyxoviridae* family. In order to limit the negative financial and social effects of the regular influenza outbreaks, The World Health Organization (WHO) monitors the pathogenicity of the different influenza strains and directs the development of the yearly vaccine. The continuous surveillance and developmental work that goes into influenza prevention could be significantly reduced if a general influenza vaccine, effective against all influenza strains, could be developed. Such a vaccine could also significantly reduce the response time in the case of an influenza pandemic. The vaccine could be distributed immediately without the need for the time-consuming process of tailoring the vaccine to the specific strain causing the epidemic. Currently, there are high hopes for using the mucosal route for vaccination as it gives a strong local and systemic immunity as well as offers easy administration [10, 11].

The work of producing a general mucosal influenza vaccine by Nils Lycke's group at Sahlgrenska University Hospital has yielded a promising vaccination compound candidate called CTA1-3M2e-DD which has a combined function of antigen and immunostimulatory agent [12]. Research is now in progress on improving how the vaccination compound is being delivered to maximize its efficiency. Coupling the construct to nanoparticles is an interesting option. In a collaboration between Nils Lycke and the division of Biological Physics at Chalmers University of Technology, the CTA1-3M2e-DD construct is coupled to liposomes. However, the combinatorial possibilities of liposome formulations are virtually endless while the composition is likely to significantly

affect the immune response [5-7, 13]. Furthermore, the current methodology used in developing both vaccination compounds and formulations uses rodent models to a large extent, which is time-consuming and expensive. The development process could thus be rationalized by an *in vitro* screening method to facilitate identification of promising candidates and exclusion of poor ones at an early stage and thus reduce the amount of costly animal experiments. Moreover, little is currently known about how the mode and rate of uptake of a vaccine correlates to its efficiency. An assay could thus also be used as a stepping stone towards a more rational and informed development process of vaccines.

This master's thesis project is intended to meet those needs by the development of an assay for the quantification and characterisation of the uptake of liposomal vaccine formulations by dendritic cells. The basis for the assay is imaging of liposome-cell interactions using total internal reflection fluorescence (TIRF) microscopy and epifluorescence microscopy to characterize the interaction using single particle tracking (SPT).

2 THEORETICAL BACKGROUND AND LITERATURE REVIEW

2.1 TECHNIQUES USED

2.1.1 Total Internal Reflection Fluorescence Microscopy

Total internal reflection fluorescence microscopy is a surface-confined technique where only the volume within the first hundreds of nanometres from the surface is illuminated. The shallow field of illumination in TIRF microscopy is achieved by using a greater angle of the incident light, Θ, than that used in traditional microscopy, which leads to total internal reflection (TIR) of the light. This results in the formation of an exponentially decaying evanescent field [14]. In order for TIR illumination to occur, the incident angle of the light has to exceed the critical angle, given by Snell's law:

$$\Theta_c = \sin^{-1}\frac{n_1}{n_2} \tag{1}$$

where n_1 is the refractive index of the sample and n_2 is the refractive index of the cover slip. Another condition for TIR is that the refractive index of the coverslip must exceed that of the sample [15], which makes glass a suitable choice of material due to its high refractive index.

The limited region of illumination means that few fluorophores are excited beyond the reach of the evanescent field which leads to a very low background fluorescence as well as reduced cellular damage when living samples are studied [14, 15]. A visual representation of TIRF microscopy is found in Figure 1.

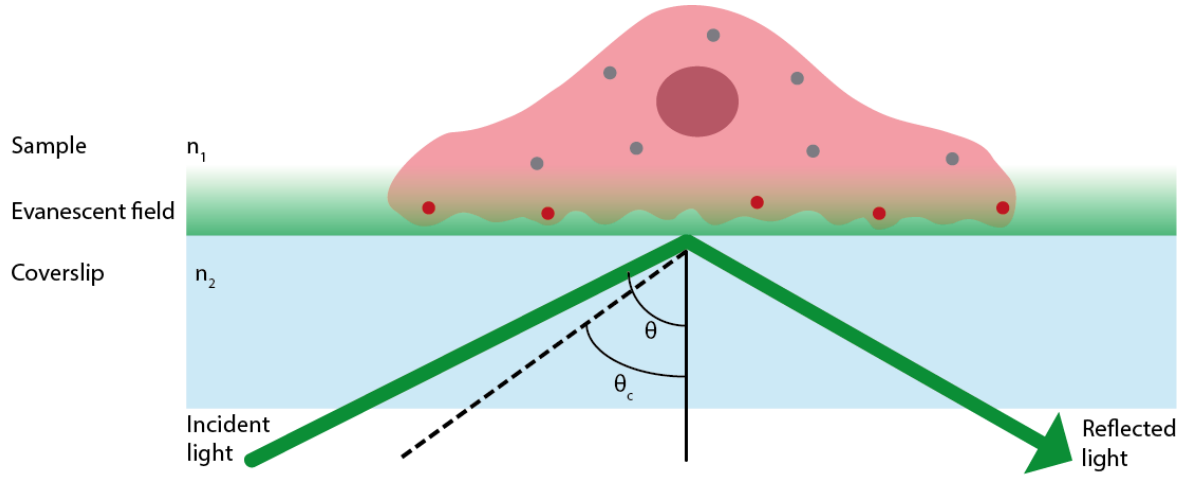

Figure 1. In TIRF microscopy the angle of the incident light, Θ, is greater than the critical angle, Θ_C, which gives rise to an exponentially decaying evanescent field. For this to occur, the refractive index of the surface, n_2, must exceed n_1, which is the refractive index of the sample.

2.1.2 Single Particle Tracking

SPT enables the study of the uptake and expulsion kinetics of individual particles by cells. It can also be used to elucidate involvement of certain molecules or components in cellular trafficking events [16-20].

SPT has been used in combination with a multitude of different microscopy techniques to study the uptake of single particles by cells [16-18, 20, 21]. The advantage of using TIRF microscopy with SPT is that TIRF microscopy effectively minimizes the background noise so that the contrast between the fluorescently labelled particles is increased compared to epifluorescence imaging, simplifying tracking of the particles.

2.2 Previous Studies of Individual Particle Uptake

The abovementioned techniques have been used separately and in combination for the study of particle uptake. The studies that are most relevant for this work are found summarized below. An example of the use of TIRF and epifluorescence microscopy in uptake studies is the work by Mattheyses *et al*. [22] who utilized the technique to study the involvement of dynamin and clathrin in endocytosis. They observed single events of scission and internalization of vesicles loaded with epidermal growth factor receptor (EGFR) tagged with green fluorescent protein (GFP). The uptake studies took place in cells expressing fluorescently labelled dynamin and clathrin and uptake was confirmed by the simultaneous disappearance of colocalized EGFR and clathrin or dynamin from the field of view. Schmidt *et al*. [19] studied the fusion of individual vaccinia virions to HeLa cells using TIRF microscopy in combination with a microfluidic device acting as a cell trap. The viruses were labelled with a self-quenching concentration of octadecyl rhodamine B chloride (R18) and the virus cores were GFP-tagged. A reduction of the pH was used to induce fusion which caused dequenching of the R18 simultaneous to reduction of the GFP signal due to internalization of the virus core. Van der Schaar [16] *et al*. studied the uptake of Dengue virus using real-time multi-colour fluorescence microscopy in combination with SPT. The virions used were labelled with self-quenching concentrations of DiD which caused them to fluoresce enough to be visualized and membrane fusion to be identified by increased fluorescence due to dequenching. Simultaneous tracking of virions and fluorescently labelled endocytic markers allowed elucidation of both the clathrin-mediated internalization and the endocytic trafficking of the Dengue virus. In continuation, Chu *et al*. [17] used confocal microscopy and SPT to confirm the interaction between DiD-labelled Dengue virus and GFP-tagged autophagosomes during early infection. Jin *et al*. [20] utilized the inherent photoluminescence of single walled carbon nanotubes to enable use of SPT to determine the uptake and expulsion rates for nanotubes of different lengths. A perfusion system was used to ensure that only nanotubes attached to the

cells were present and a camera with 295 nm depth of field ensured that only the cross section in focus was observed. de Bruin *et al.* [18] used wide-field fluorescence microscopy and SPT to study the uptake of polyplexes functionalized with EGF in order to target EGFR. The extracellular Cy3-labelled EGF polyplexes were selectively quenched with Trypan blue to quantify the amount taken up, as well as to establish that the uptake took place during a certain movement phase identified with SPT. Tian *et al*. [23] studied the movement of exosomes in medium, on the cell surface and in the cytosol using real-time fluorescence microscopy and used Trypan blue to distinguish between intra- and extracellular DiI-labelled exosomes. Furthermore, SPT was used to identify distinctly different movement patterns in freely diffusing and membrane-bound exosomes. Aaron *et al*. [21] used TIRF microscopy in combination with SPT to study the uptake behaviour of immune cells subjected to quantum dots of different shapes. SPT was used to determine the average diffusion coefficient and the uptake was quantified by measuring the overall decrease in fluorescence as the quantum dots disappeared from the field of view when taken up. In summary, the different phases of a particle uptake process are generally distinguished using co-localization of a dye pair, selective extracellular quenching and/or an observable shift in the movement behaviour of the particle.

2.3 VACCINES AND THE IMMUNE SYSTEM

Vaccines can roughly be divided into two groups: live attenuated and non-living vaccines which include inactivated whole-cell, subunit vaccines and conjugate vaccines. Live attenuated vaccines are based on the use of living bacteria or viruses with reduced virulence compared to the pathogenic original strain. Inactivated whole-cell vaccines consist, as the name suggests, of intact but non-living bacteria or viruses. Subunit vaccines are made up of components of cells or viruses, such as membranes, proteins or polysaccharides [10, 11]. Conjugate vaccines, such as the CTA1-3M2e-DD construct, combines a weak antigen with a component that will enhance the immune response. The highly effective vaccines against polio [10], measles and smallpox, among others, are examples of live attenuated vaccines that are familiar to most of us [24]. A single dose of a live attenuated vaccine is often enough to provide lifelong protection and the acquired immunity closely resembles that of someone who has survived an actual infection [24]. However, the live attenuated vaccine approach is not effective for all diseases. This is typically the case for rapidly mutating diseases like HIV and diseases like malaria, where having been infected once does not protect from future infections. Additionally, there are also stability and safety issues associated with this type of vaccines. Since they consist of live specimens, there is a risk that the attenuated strain reverts back to the pathogenic wild type and the balance between sufficient immunogenicity and attenuation is always an issue [10]. There are fewer concerns for the safety of non-living vaccines, but they are less effective at inducing an immune response and the

resulting protection is often transient, making repeated administration a necessity. Adjuvants, immunostimulatory agents, are therefore co-administered to improve and direct the response. There are however very few adjuvants currently licensed for use [24]. Interestingly, despite centuries of use and decades of research, most current vaccines and adjuvants are developed empirically with little consideration for the underlying mechanisms [24].

Generally speaking, the immunization process starts when an antigen (from a pathogen or a vaccine) is captured by an antigen-presenting cell (APC). There are several types of APCs but the primary immune response can only be induced by dendritic cells [25]. Once the antigen has been taken up using one of several modes of uptake available to dendritic cells, the cell will begin to mature. It will rapidly lose its ability to capture antigens and instead assemble complexes with the antigen and major histocompatibility complex (MHC) class II and display them on the cell surface [26]. These complexes are recognized by and activate $CD4^+$ T helper cells. Activated T helper cells release cytokines which activate the B cell immune response with subsequent antibody release [11]. In contrast, cells that are expressing viral antigens due to infection display them on the surface in complex with MHC class I, which instead activates $CD8^+$ T cells to become cytotoxic T-lymphocytes [11, 26].

The point of entry for most pathogens is through the mucosa and it is therefore desirable to activate the local immune system in these tissues [11]. Mucosal vaccines trigger humoral and cell mediated immunity at mucosal sites but also systemically with long-term B and T cell memory [10]. In fact, mucosal administration of vaccines is the only possibility to effectively activate the cell-mediated defence locally in the mucosa [10]. Upon vaccination, dendritic cells are activated, which results in migration from the mucosal tissues to the draining lymph nodes where they activate the mucosal homing properties of B and T cells. The antigen-activated B and T cells then travel with the blood stream to mucosal tissues [10] where they act as an early line of defence against infection. Another fact that speaks for the importance of activating the cell-mediated immunity is that T cell responses have been shown to be a better indicator than antibody titres for predicting susceptibility to infection following vaccination [27].

In spite of the recognized potential of mucosal vaccination strategies, and of the fact that parenteral vaccines administrated subcutaneously or intramuscularly will likely create a strong systemic, antibody-mediated response and only a weak cell-mediated response [28], mucosal administration has to date failed to become common globally. A contributing reason for this is that this strategy is generally less effective in developing countries [10]. Nutritional deficiencies and parasitic infections impairing or skewing the mucosal immune system are possible causes for this effect and treatment of underlying infections might be a way of increasing the efficacy of mucosally administered vaccines [10]. Furthermore, the anatomy of the mucosal routes makes

successful vaccination technically challenging. For intranasal and inhaled vaccines the mucosal barrier and the mucociliary clearance system constitute obstacles for efficient delivery. In the oral route, the tight junctions between cells are designed to prevent passage, and the high enzymatic activity in the gastrointestinal tract degrades vaccines [11]. Generally speaking, the bioavailability is low for oral vaccines and the lack of control over the dose that is actually taken up is problematic [29]. Repeated administration or high doses are often required to produce lasting protection; high doses can however lead to systemic tolerance. Another obstacle to fast and efficient vaccinations using mucosal vaccines is the compartmentalization of the mucosal immune system. This phenomenon means that if a mucosal vaccine induces a strong immune response at the site of administration, it does not necessarily induce strong protection in other mucosal tissues [11].

Nevertheless, mucosal vaccines are still considered highly interesting in a number of applications as they offer other advantages apart from their ability to efficiently modulate a part of the immune system only poorly activated by parenteral vaccines. Mucosal vaccines are generally both more economical and safer compared to parenteral vaccines; the risk of transferring blood-borne infections is diminished as no needles are necessary. Furthermore, mucosal vaccines can be administered by personnel without medical training [10, 30] which would be especially useful in the case of a pandemic [10, 11]. The mucosal immune system has a high activation threshold as it is located in close proximity to areas with an abundant natural bacterial flora. The gastrointestinal tract is a good example of where the immune system cannot be too sensitive due to the large number of beneficial bacteria present [30]. Purity is hence far less important for mucosal than for systemic vaccines but the high tolerance also makes it challenging to formulate efficient mucosal vaccines and finding safe and efficient adjuvants is crucial.

2.4 Carriers for Vaccination Compounds

Particles such as liposomes, polymeric nanoparticles and virus-like particles can have adjuvanting properties in addition to the advantages of acting as carriers for vaccination compounds, drugs and other active molecules [6]. Particulate carrier systems have gained increasing interest as a way of altering the pharmacokinetics and biodistribution of compounds as well as a way to achieve prolonged release [1]. Such systems typically consist of carriers in the form of micro- or nanoparticles which can effectively increase the bioavailability and reduce the toxicity of a compound, allowing for administration of higher doses and widening of the therapeutic window. Carriers also open up for the possibility of targeting specific tissues and/or cells as well as controlling the release in order to produce a prolonged immune response [6]. Another advantage of using carriers over other adjuvants is the possibility to tailor them so that the loaded proteins are released intracellularly. It has been shown that intracellular release

allows for activation of the MHC class I pathway which is normally unavailable for exogenous proteins and which triggers a cytotoxic T lymphocyte response [5, 31].

Particulate carrier systems consist of spheres or capsules and can, generally speaking, be polymer-, lipid- or metal-based [11]. Many different synthetic polymers have been used for nanoparticle production but notable examples are poly(lactic acid) (PLA) and poly(lactic-co-glycolic acid) (PLGA) which are biodegradable and have been extensively used for implant and controlled drug release purposes [11, 29]. Examples of natural polymers used for vaccine administration applications are chitosan, collagen, alginate and gelatine [29]. Furthermore, a variety of delivery systems including emulsions, co-polymer micelles, dendrimers, [29] carbon nanotubes [32] as well as nanoparticle-in-microsphere formulations have been considered. Highly interesting candidates with current applications in both drug and vaccine delivery are liposomes which are innately biocompatible and biodegradable when lipids found in the native cell membrane are used [7]. Antigens with different properties, like proteins, carbohydrate, nucleic acids and haptens can all be used with liposomes since hydrophilic compounds can be transported in the aqueous core while hydrophobic compounds can incorporate into the lipid bilayer. There is also the possibility to couple compounds to the surface [5-7]. Surface-grafting has been used for example to attach antibodies, peptides and folate for cell targeting [5]. Furthermore, there are practically endless possibilities for customization of the physicochemical properties of the liposomes which have inherent immunological adjuvanticity [5, 6]. Lipid composition, size, surface charge [13] and functionalization [6, 7] as well as membrane fluidity all affect the immune response [6, 33] and can be tailored to suit the application of interest. The adjuvanticity can further be enhanced and manipulated by the use of novel immunostimulatory lipids [7] and constituents from virus membranes [5, 7]. It is also possible that the lamellarity of the liposomes has an effect on the immune response even if this is difficult to prove since production of liposomes with similar composition but different lamellarity involves different preparation methods [6]. The mechanisms responsible for the adjuvanticity of liposomes are not completely elucidated. Positively charged liposomes have been shown to interact electrostatically with the negative mucosa-associated lymphoid tissue, providing time for antigen sampling and immune cell activation. Cationic liposomes also get internalized by dendritic cells to a large extent, possibly due to interactions with negatively charged proteins on the cell surface. Another theory is that of passive targeting, which hypothesizes that liposomes are well-suited for delivery of pathogen-associated molecules due to their similar size and shape to many pathogens, allowing for easy uptake by antigen-presenting cells [6].

Different types of drug delivery systems are specifically advantageous for mucosal administration. Orally administered peptides and proteins are not stable in the harsh

environment of the gastrointestinal tract and polymeric nanospheres or –capsules [29] as well as liposomes [5, 6] provide protection from external conditions as well as the possibility to target and control the release. Furthermore, liposomes increase the uptake rate through biological membranes [6]. For nasal and inhaled vaccines, rapid mucociliary clearance is an obstacle to sufficient activation of the immune system [11]. Illum *et al*. uses chitosan-based bioadhesive systems in order to slow down the clearance rate and achieve longer contact between the vaccine formulation and the tissues of the nasal cavity [34]. The positively charged polysaccharide chitosan interacts strongly with negatively charged materials such as cell surfaces and mucus which significantly increases clearance time. Chitosan has also been proven to directly increase uptake by stimulating paracellular transport by temporarily opening the tight junctions between cells [34]. Chitosan can in fact induce an immune response on its own when administered orally and has, like poly(ethylene glycol) (PEG), been used to increase the interaction of less hydrophilic materials with the mucosa [29]. Coupling of PEG and other hydrophilic polymers to liposomal membranes is commonly used in order to increase the circulation time of the liposomes [5, 33]. Such surface modification creates an extra hydration layer which delays opsonisation [5] and subsequently phagocytic clearance [33]. In addition, research is being done in order to attach PEG in a detachable fashion in order to later allow cells to capture the liposomes [5]. Vila *et al*. [35] have shown that coating hydrophobic polymer nanoparticles with a hydrophilic compound, such as PEG or chitosan, causes a significant increase in uptake when administered orally or nasally. In order to transport large molecules, proteins and particles across the lipophilic barrier that the cell membrane poses, cell-penetrating peptides can be used. Such peptides have been shown to significantly increase uptake and provides a way for exogenous proteins to enter the cytosol and activate the MHC I processing pathway [36]. Josephson *et al*. [37] showed that cell-penetrating peptides increase the lymphocyte internalization of particles with mean size of 41 nm 100-fold compared to non-modified particles. Cell-penetrating peptides have also been showed to increase intracellular delivery of liposomes [36].

In short, there are many different promising carrier systems and a multitude of ways to tailor them in order to achieve the efficient, directed delivery and immune system activation that is required in order to produce effective mucosal vaccines for preventing the emergence of new, devastating pandemics.

2.5 INFLUENZA A

Throughout the 20th and 21st centuries, influenza A has caused numerous outbreaks, ranging in severity from the seasonal flu to the pandemic Spanish influenza which caused the deaths of at least 40 million people in 1918-1919 [38]. Aquatic birds are thought to be the origin of the virus

but it has later evolved to infect other animals, including various birds, sea mammals, horses, pigs and humans [39]. Influenza A is distinguished from the related B and C types by differences in their matrix protein and nucleoprotein. Influenza A strains are further categorized based on which of the 16 different haemagglutinin (H1-H16) and 9 different neuraminidase (N1-N9) surface glycoproteins they possess [38]. Haemagglutinin is the main antigen towards which the host produces antibodies [40] and is involved in virus-cell binding and fusion by interacting with the sialic acid of receptors on the host cell surface. Neuraminidase cleaves heamagglutinin from sialic acid which enables the virion to enter and exit the host cell [40].

Antigenic drift, random mutations in the antigenic sites, mainly in certain epitopes of haemagglutinin, is considered responsible for the seasonal influenza returning each year and circumventing the acquired immunity of previous infections. The outbreaks of seasonal influenza due to these minor genetic changes of the virus are costly as they cause 3 to 5 million cases of severe illness and 250 000 to 500 000 deaths yearly [41]. Larger genetic changes in the influenza A virus, so-called antigenic shifts, occur approximately 3 times per 100 years and generally give rise to serious epidemics [42]. These relatively rare outbreaks have proven to be potentially disastrous with higher infectivity and pathogenicity than the seasonal influenza. Antigenic shift occurs when a host cell is infected by different virus types, giving rise to so called reassortants, combination viruses which have acquired genes of mixed origin through segment reassortment [38, 40]. The process of antigenic shift is accredited with the development of virus types capable of cross-species infection as a very large number of random mutations are required to enable infection from one species to another [40]. A reassortant that expresses antigenic surface glycoproteins of a different origin than its host species will be able to bypass the immune system, effectively increasing the infectivity of the virus. A variety of influenza A virus types circulate simultaneously among pigs and the virus that caused the swine influenza pandemic of 2009 was generated from a mixture of several strains [43]. Furthermore, all but one of the viruses causing the pandemics of the 20th century had acquired haemagglutinin of avian origin [38]. Since 1997, influenza viruses of purely avian origin have been transmitted directly from birds to humans, raising concerns over the possible emergence of a new, severe influenza pandemic [38].

The WHO monitors the changes of the ever evolving influenza strains in both humans and animals with the goal of keeping the yearly vaccines updated [42, 44]. Twice yearly, in February for the northern hemisphere and in September for the southern, the WHO reviews which strains are likely to cause disease the following winter season [44]. The assessment of the WHO is the basis of the composition of the next influenza vaccine and companies have approximately 6 months to develop and produce the vaccine [44]. The viruses do however not cease to evolve from the time of the WHO's sampling up until the influenza outbreak of the following season. Significant changes

in the virus antigens that take place during this window render the vaccine less effective and may leave an opening for the outbreak of an epidemic [42]. Considering the changeable nature of influenza A and the likely sudden outbreak and fast progress of a future pandemic, an ideal vaccine would be based on a virus component present in all strains. The vaccine could then be developed before the actual outbreak of the next pandemic and be optimized for the demands on ease of administration and transport of a mass vaccination. A step towards such a vaccine is the vaccination construct that combines the function of adjuvant and antigen developed by Eliasson *et al*. [12]. The fusion protein called CTA1-3M2e-DD consists of an adjuvant comprising a dimer of a portion of *Staphylococcus Aureus* protein A as well as the ADP-ribosylating A1 portion of the cholera toxin (CTA1). The CTB portion of the cholera toxin is not included in order to avoid toxic effects while still maintaining high adjuvanticity [45]. The antigen region consists of three repeats of M2e, the highly conserved external part of matrix protein 2, which is found in the membrane of all human influenza A virus strains [12].

The work described in this master's thesis is aimed towards providing a useful tool in the development of a delivery vector for the CTA1-3M2e-DD construct.

3 AIM

The objective of this master's thesis project is the development of an assay for the study of uptake of functionalized liposomes by dendritic cells. The intention is to characterize the particle uptake by visualizing initial attachment of liposomes to cells, their movement on the cell surface and finally, individual uptake events. The characterization is done using single particle tracking of time lapses acquired by fluorescence microscopy. As detailed in section 4, we have tested and evaluated different experimental approaches towards this aim. We take advantage of the surface confined illumination of TIRF microscopy in order to limit the imaging to the basal membrane and visualize the particle movement with high sensitivity. Epifluorescence imaging is further used in an attempt to study the change in number of particles attached to the cell membrane over time, in order to make a general quantification of the uptake.

4 OVERVIEW OF THE EXPERIMENTAL APPROACHES

4.1 CHOICE OF CELL TYPE

Dendritic cells play a central role in the overlap between the innate and adaptive immune systems [30] (see section 2.3). Furthermore, they are important targets for adjuvants in general [10, 30] and specifically for the immunostimulatory part of the CTA1-3M2e-DD construct [10]. In view of these facts, a dendritic cell line was selected for this project. Specifically, a fetal skin dendritic cell (FSDC) line derived from mouse [46] was used, as robustness and ease of handling was a priority during the initial development. The optimized assay could later be carried out with primary cells in order to get biological information as relevant as possible, and to ensure a parallel between the data obtained *in vitro* and the data generated *in vivo.*

4.2 ASSAY SETUPS

To achieve the abovementioned aims the following experimental procedures were evaluated:

A) *Addition of liposomes to adhered cells:* In the first and most basic approach, cells were first allowed to adhered to a glass surface. Liposomes were then added in anticipation that they might diffuse under the cells to be taken up through the basal membrane, in addition to the unhindered uptake through the apical membrane. Single particle tracking was done to characterize the short-term movement of liposomes on the cell surface (Figure 2A).

B) *Mixing liposomes with cooled, detached cells:* Cells and liposomes were mixed in solution while cooling on ice in order to make the cell membrane stiff, allowing liposomes to distribute and attach evenly around the cells while postponing the uptake process [21]. Cells were then allowed to settle and adhere to a glass surface where they were warmed in order to restore fluidity to the membrane and allow uptake to be imaged at the basal membrane. This procedure was selected in an attempt to facilitate access of the liposomes between the substrate and the basal cell membrane. Single particle tracking was done to characterize the short-term movement of liposomes on the cell surface (Figure 2B).

C) *Addition of liposomes to cooled, adhered cells:* Cells that had adhered to glass overnight were incubated with liposomes on ice to allow liposome attachment to the cell membrane while delaying uptake. Excess liposomes were rinsed off and the cells were warmed to restore fluidity to the membrane to allow liposome uptake. Quantification of uptake was attempted by observing the change in the number of liposomes attached to the cell surface over time (Figure 2C).

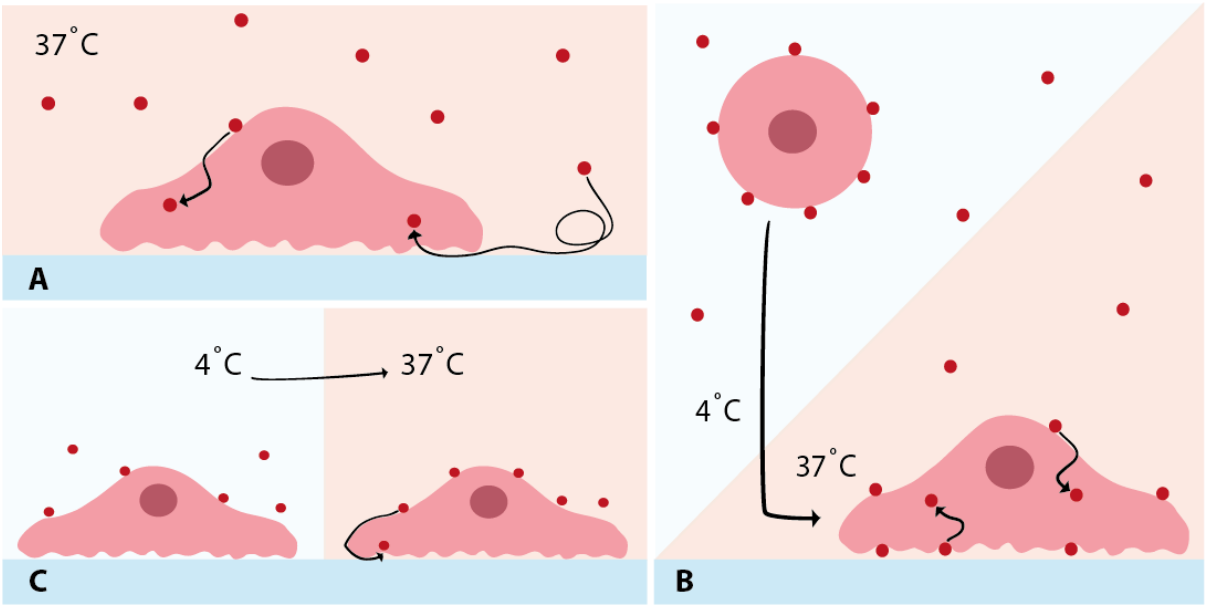

Figure 2. In approach A, liposomes were added to adhered cells to investigate whether liposomes would diffuse between the cell and the surface, allowing imaging with total internal reflection fluorescence (TIRF) microscopy and single particle tracking (SPT). In approach B, detached cells were incubated with liposomes on ice in order to allow liposomes to attach to the cell surface and be present between the cell and the surface when the sample was warmed, allowing TIRF microscopy imaging and SPT. In approach C, adhered cells were incubated with liposomes on ice to allow attachment while delaying uptake. The sample was subsequently rinsed in order to remove excess liposomes. Uptake was quantified by monitoring the change in the number of liposomes attached to the cell surface using epifluorescence microscopy.

5 MATERIALS AND METHODS

5.1 CELL CULTURE

FSDCs, kindly provided by Nils Lycke at Sahlgrenska University Hospital, were cultured at 37°C and 5 % CO_2 in Iscove's Modified Dulbecco's Medium (IMDM) (Thermo Scientific, USA) supplemented with 10 % fetal bovine serum, L-glutamine, 2-mercaptoethanol and gentamicin. Non-enzymatic harvesting was done using cell scrapers (BD Falcon, USA).

5.2 SETTING UP THE LIVE CELL MICROSCOPY

Initially, the basic set-up for the live cell microscopy was tested and optimized in order to ensure cell growth under the imaging conditions.

5.2.1 Cell Culture on Glass Surfaces

FSDCs are normally grown on plastic substrates but glass is required to achieve TIR illumination. It was therefore tested whether the cells grew on glass or whether a coating was needed to allow normal cell growth. Glass coverslips with a diameter of 25 mm were immersed in Cobas Integra acidic cleaner (Roche Diagnostics GmbH, Germany) for 20 minutes and dried with nitrogen gas. The coverslips were cleaned by UV/ozone for 1 hour. In an attempt to enhance cell-attachment, coverslips were coated with Poly(L-lysine) (PLL) (Sigma-Aldrich, Sweden). For this, the polymer was diluted in MilliQ water to a concentration of 10 µg/ml and sterile-filtered. 5 drops of solution were then placed on each coverslip. After 20 minutes, the coverslips were rinsed with sterile-filtered MilliQ water. Cells were seeded in equal amounts on triplicates of untreated glass, glass coated with PLL, as well as directly on the plastic of a 6-well plate. Cells were imaged using a DM IL LED brightfield microscope (Leica, Germany) after 1 hour and again after 24 hours.

5.2.2 Choice of CO_2-independent Medium

IMDM, the medium generally used for culture of FSDCs, is dependent on an atmosphere containing 5 % CO_2 in order to maintain a constant, neutral pH. As imaging took place in an uncontrolled atmosphere, it was necessary to find an alternative medium to use during microscopy. Two candidates, Leibovitz's L15 (Thermo Scientific, USA) and RPMI (Thermo Scientific, USA) were compared to IMDM, all supplemented with 10 % fetal bovine serum, L-glutamine, 2-mercaptoethanol and gentamicin. 3 ml of each medium was placed in 2 wells of a 6-well plate. 400 µl cell solution was seeded in each well, giving a final concentration of 700 000 cells/well. The cells were incubated at 37°C and 5 % CO_2. After 1 hour and again after 24 hours the cells were non-enzymatically harvested from 3 wells (one of each medium type) using cell scrapers (BD Falcon, USA) and analysed using the Muse Count & Viability kit in a Muse Cell

Analyzer (Millipore, USA). 1000 cells were analysed from each sample and the ratio of living to dead cells was determined.

5.2.3 Cell Membrane Staining

A cell-membrane staining using the PKH67 green fluorescent cell linker kit for general cell membrane labelling (Sigma-Aldrich, Sweden) was performed to evaluate the possibility to determine the position of the membrane on the surface and aid identification of individual uptake events. The staining was performed according to the protocol in Appendix A, amended for use with $2 \cdot 10^6$ cells by diluting the dye stock 4 times in 95 % ethanol to 0.25 mM and using half of all volumes. In brief, the cells were washed with phosphate buffered saline (PBS: 0.01 M phosphate buffer, 0.0027 M KCl, 0.137 M NaCl, pH=7.4) and centrifuged into a pellet using a Mikro 22R centrifuge (Hettich Zentrifugen, Germany) (1500 rpm). The pellet was resuspended in 500 ml Diluent C. 2 µl of the diluted PKH67 dye was diluted in 500 µl Diluent C and mixed with the cell solution. The mixture was incubated for 5 minutes before addition of 1 ml 0.11 % bovine serum albumin. After a 1 min incubation, the cells were washed 3 times and resuspended in IMDM.

5.3 Liposome Production and Functionalization

To test liposome uptake by the FSDC cells, two types of liposomes were used: preliminary tests were performed with positively charged liposomes. In later experiments, liposomes carrying the vaccine construct were used. All lipids used to produce the liposomes were bought from Avanti Polar Lipids, USA.

The positive liposomes were produced with a 78:20:2 w/w ratio of the lipids 1-palmitoyl-2-oleoyl-sn-glycero-3-phosphocholine (POPC), 1,2-dioleoyl-*sn*-glycero-3-ethylphosphocholine (chloride salt) (POEPC) and 1,2-dioleoyl-sn-glycero-3-phosphoethanolamine-N-(lissamine rhodamine B sulfonyl) (PE-Rhod). 1 mg of lipids were placed in 500 µl of chloroform-methanol mixture (50:50, v/v) in a round-bottom flask. The solvents were evaporated under a flow of nitrogen gas to form a thin lipid film. Traces of solvents were removed by keeping the round flask under vacuum for a minimum of 1 h. The lipid film was rehydrated in 1 ml PBS. The suspension was extruded 11 times through a 30 nm nucleopore track-etch polycarbonate membrane (Whatman, UK).

To prepare liposomes to be functionalized with the vaccination construct a lipid film containing a 80:10:8:2 w/w ratio of POPC, 1,2-dioleoyl-sn-glycero-3-phosphoethanolamine-N-[4-(p-maleimidomethyl)cyclohexane-carboxamide] (PE-MCC), cholesterol and PE-Rhod was produced as described above. The lipid film was rehydrated in 1 ml of sodium acetate saline buffer (10 mM sodium acetate, 150 mM NaCl, pH=5). The suspension was extruded 11 times through a 100 nm

nucleopore track-etch polycarbonate membrane (Whatman, UK). Traut's reagent (2 µl of a 0.9 mM solution in 10 mM PBS, $1.8 \cdot 10^{-9}$ mol) was added to a CTA1-3M2e-DD construct solution (32 µl of a 35 µM solution in 10 mM PBS, $1.1 \cdot 10^{-9}$ mol) and allowed to react for 20 minutes at 4°C. Liposomes composed of POPC/PE-MCC/cholesterol/PE-Rhod (80:10:8:2) (50 µl, $0.5 \cdot 10^{-8}$ moles of PE-MCC) were added to the freshly thiolated construct and incubated for 1 hour at 4°C. The unreacted thiolated construct was removed from the functionalized liposomes using a 100kDa cut-off (Millipore, USA) centrifugal filter after a 3 minute centrifugation at 8000 rcf.

The liposomes used in section 5.4.3 were functionalized as described above, using 0.75 µl of 1.5 mM Traut's reagent in PBS ($10.9 \cdot 10^{-9}$ mol), 16 µl of 35 µM CTA1-3M2e-DD construct in PBS ($5.6 \cdot 10^{-10}$ mol), and 25 µl POPC/PE-MCC/cholesterol/PE-Rhod (80:10:8:2) liposomes ($0.25 \cdot 10^{-8}$ moles of PE-MCC).

5.4 Sample Preparation and Fluorescence Microscopy

Incubation chambers were prepared by rinsing custom-made polydimethylsiloxane (PDMS) (Dow Corning Corporation, USA) rings in 70 % ethanol and allowing them to air dry. Glass coverslips with thickness number 1 were rinsed in 70 % ethanol and dried with nitrogen gas. Incubation chambers were assembled by repeatedly pressing adhesive tape to the bottom of the PDMS rings and subsequently attaching them to glass coverslips.

Imaging was done using a Ti Eclipse with a 60x oil TIRF objective (Nikon, Japan) and an Ixon DU-987E cooled CCD camera (Andor, UK). The temperature of the samples was controlled using a PDMI-2 open perfusion microincubator with a TC-202a bipolar temperature controller (Harvard Apparatus, USA).

5.4.1 Addition of Liposomes to Adhered Cells

Cells were seeded in IMDM with a concentration of 250 000 cells/ml in an incubation chamber, 24 hours prior to imaging, and incubated at 37°C and 5 % CO_2. The cells were, at the time of seeding, treated with 2 µl recombinant IFN-γ per 3 ml cell solution to increase the endocytic activity. Prior to imaging, the sample was rinsed once with PBS and 400 µl Leibovitz's L15 medium with Phenol Red, supplemented with 10 % fetal bovine serum, L-glutamine, 2-mercaptoethanol and gentamicin. 2 µl of liposome solution with a concentration of 0.1 mg/ml was added to the 400 µl of medium in the incubation chamber and the solution was mixed by pipetting gently. Time-lapses consisting of 1000 images taken every 0.2 seconds were acquired every 10 minutes over 2 hours.

5.4.2 Mixing Liposomes with Cooled, Detached Cells

Cells were seeded in IMDM with a concentration of 250 000 cells/ml in a 35 mm diameter petri dish, 24 hours prior to imaging, and incubated at 37°C and 5 % CO_2. Samples to be used with functionalized liposomes were, at the time of seeding, treated with 2 µl recombinant IFN-γ per 3 ml cell solution to increase the endocytic activity. Prior to imaging, cells were non-enzymatically harvested using cell scrapers. The solution was transferred into two 1.5 ml eppendorf tubes and centrifuged (5 minutes at 2000 rpm). The supernatant was removed and one pellet resuspended in 500 µl cold (4°C) medium supplemented with 10 % fetal bovine serum, L-glutamine, 2-mercaptoethanol and gentamicin. Both IMDM and Lebovitz'z L15 was used. 200 µl medium was added to a PDMS/glass well before focusing the microscope at the glass surface. 2 µl 0.1 mg/ml liposome solution were mixed with 200 µl of the cell solution and added to the incubation chamber. The sample was cooled in the microincubator for 20 minutes before the temperature was raised to 37°C. The first time-lapse was taken 15 minutes after initiation of warming and time-lapses with a total of 1000 images taken every 0.2 seconds were acquired every 10 minutes over a period of 2 hours.

5.4.3 Addition of Liposomes to Cooled, Adhered Cells

Cells were seeded in IMDM with a concentration of 250 000 cells/ml in an incubation chamber 24 hours prior to microscopy. The cells were incubated at 37°C and 5 % CO_2. The sample was placed on ice, rinsed once with cold PBS and 400 µl cold Leibovitz's L15 without serum and Phenol Red was added. 2 µl 0.3 mg/ml functionalized liposome solution was added and the solution was mixed and incubated on ice for 30 minutes. The sample was rinsed 5 times with 300 µl warm (37°C) PBS, always leaving 100 µl fluid to cover the cells and avoid drying. 300 µl warm Leibovitz's L15 was added and 1000 images were taken 3 seconds apart.

5.5 Single Particle Tracking

Single particle tracking is generally performed by initially applying an intensity threshold to separate particles from background noise. A 2D Gaussian function is fitted to the intensity profile of each particle which enables position determination of the particles with an accuracy far exceeding the optical resolution. The trajectories are subsequently determined using a nearest-neighbour algorithm and the mean-square displacement is calculated which is in turn used to characterize the type of movement the particles are exhibiting [47]. In this case, particles were tracked using a dedicated MATLAB script created by Stephan Block at the division of Biological Physics, Chalmers Technical University (S. Block, personal communication, 2014).

5.5.1 Counting of Liposomes

In order to evaluate the change in number of attached liposomes over time in the images obtained from the approach described in section 5.4.3, a MATLAB script kindly provided by Stephan Block was used (S. Block, personal communication, 2014). The original script identified the number of particles in individual images by finding localized intensity maxima, with an intensity threshold to exclude the insignificant peaks. It was modified to be used with time-lapses and the threshold level was set individually for each cell based on the intensity levels at the end of the time-lapse. The data was binned into 11 data points prior to plotting.

6 RESULTS

6.1 SETTING UP THE LIVE CELL MICROSCOPY

In the first step towards setting up the assay, working conditions for live cell microscopy were tested to ensure that the cells are not adversely affected by conditions that differed somewhat from regular cell culture. This is important to ensure that the data obtained with the assay is relevant and not skewed due to unhealthy cells.

6.1.1 Cell Culture on Glass Surfaces

As mentioned in section 2.1, glass is the substrate of choice for use with TIRF microscopy as a high refractive index is required. Normally, FSDCs are cultured on plastic. A test culture was therefore done to determine whether the cells would grow on glass and whether coating of the glass substrates would be necessary. Cells were cultured on uncoated glass, glass coated with PLL and in standard plastic petri dishes. The cells were observed after 1 and 24 hours to assess their growth and morphology. As seen in Figure 3, no distinct differences between the number of cells and their morphology in the different cases could be established. Uncoated glass was therefore used for the analysis as it simplified the preparation of the incubation chambers used for microscopy.

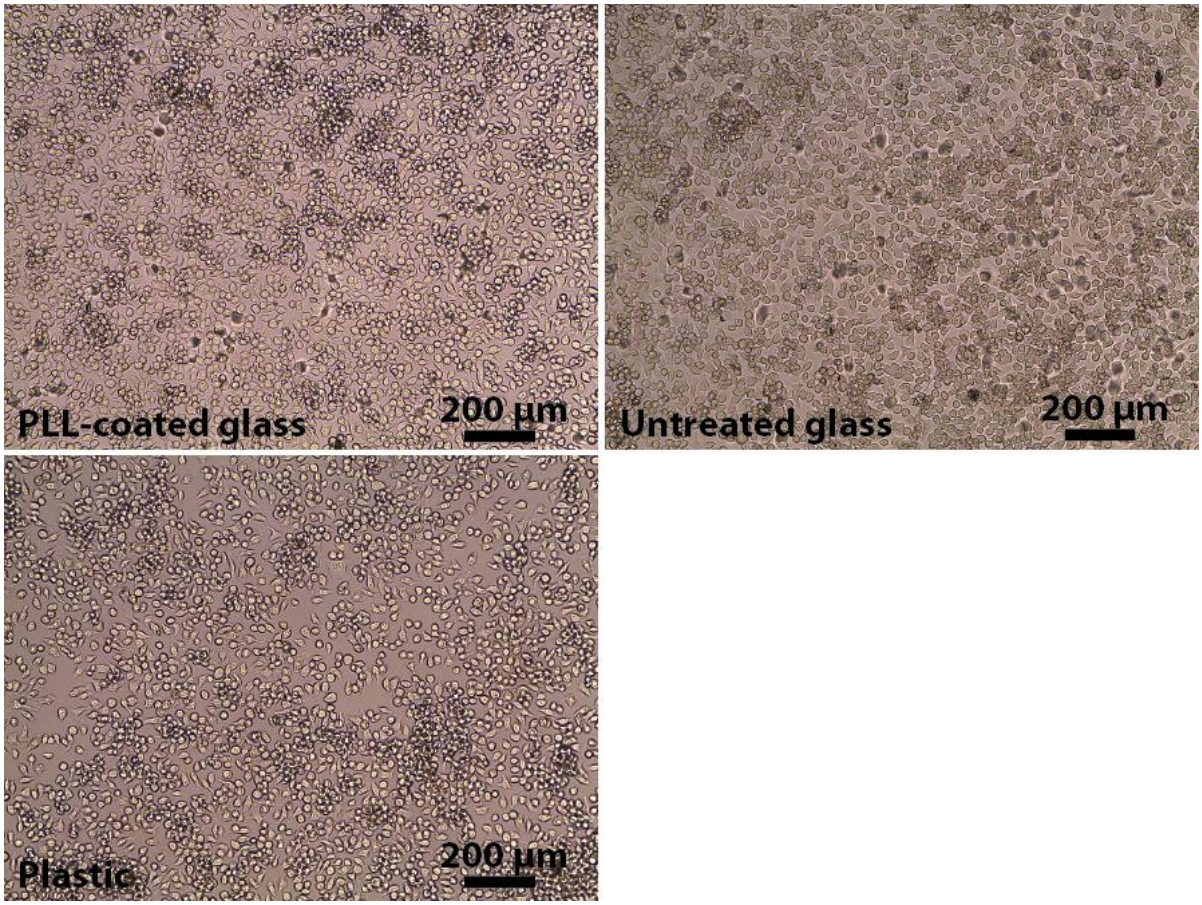

Figure 3. The images show FSDCs cultured 24 hours in complete IMDM on different surfaces.

6.1.2 Choice of CO_2-independent Medium

Live cell imaging was performed in an uncontrolled atmosphere. The standard FSDC culture medium, IMDM, is a CO_2-dependent medium buffered with sodium bicarbonate. The use of IMDM as an imaging medium would therefore lead to a decrease in pH over time. The use of a CO_2-independent medium is thus advisable. In order to select a CO_2-independent medium suitable for the particular cell line used, cells were cultured in IMDM and the two candidates Leibovitz's L15, which is a CO_2-independent medium without a sodium bicarbonate buffering system and RPMI, which does have a sodium bicarbonate buffering system, but is believed to work in short term cultures. Cell viability was measured using flow cytometry, 3 hours after seeding and again after 24 h. As can be seen in Table 1, neither of the candidates appeared to have a detrimental effect on the cells as both media yielded a larger number of viable cells than the IMDM. Leibovitz's L15 was chosen for the live cell imaging as it is a medium specifically designed for use in environments with uncontrolled CO_2-levels and would thus probably give a more stable environment during longer experiments.

Table 1. Portion of viable cells from the analysis of medium candidates for live cell imaging using the Muse Count & Viability kit.

Medium type	Viable cells after 3 h (%)	Viable cells after 24 h (%)
IMDM	62.2	76.2
Leibovitz's L15	72.6	83.7
RPMI	75.9	81.0

6.1.3 Cell Membrane Staining

In the initial experiments, a membrane staining protocol was evaluated to be used as a way of determining the position of the cell membrane in relation to the liposomes. Since the liposomes were labelled with rhodamine, which has excitation and emission wavelengths at 560 and 583 nm, respectively, the green fluorescent dye PKH67, with excitation and emission wavelengths at 490 and 502 nm was used for the membrane staining. Theoretically, the membrane stain could be used to confirm the position of the cell and that the membrane is in close proximity to the glass surface, facilitating the evaluation of whether the liposomes have been taken up. An initial test was performed to evaluate how well the membrane stain fulfilled this objective. The test revealed that the PKH67 stain gave an uneven, grainy appearance as seen in Figure 4. The brighter spots could be the locations of focal adhesions, where the membrane comes very close to the surface. They could however also be a sign that the membrane stain is internalized and that the spots seen are intracellular vesicles. The uncertainty regarding the destiny of the dye makes it a poor means for determining the position of liposomes as being intra- or extracellular. Membrane staining was therefore not implemented in the assay.

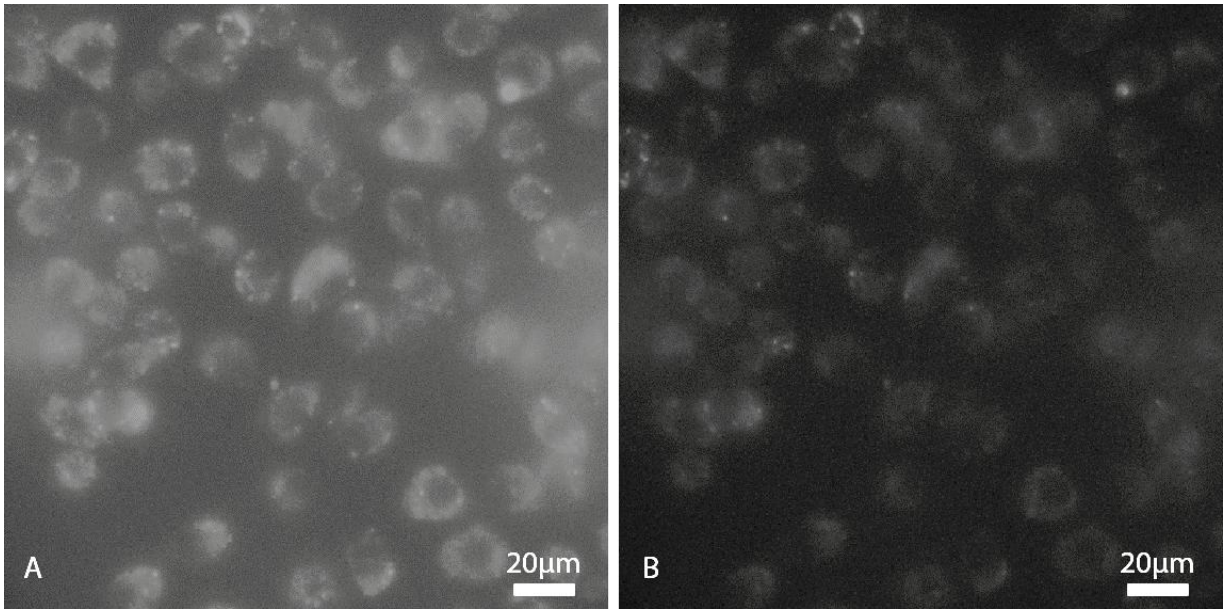

Figure 4. Images show PKH67-stained FSDCs in complete IMDM. Image A is taken using epifluorescence illumination and Image B is taken using TIR illumination.

6.2 Addition of Liposomes to Adhered Cells

The most basic approach to visualize particle attachment, movement and uptake by the FSDCs used in the study, was the addition of liposomes to surface-adhered cells, as schematically shown in Figure 2A. It was uncertain whether the liposomes would diffuse between the cells and the glass substrate. It was therefore necessary to evaluate whether it is possible to image liposomes on the basal membrane of FSDCs using TIRF microscopy and whether the acquired images are of high enough quality to allow SPT. The images in the left column of Figure 5 demonstrate that individual fluorescent liposomes attached to the underside of the cell can be clearly visualized by TIRF microscopy. Single liposomes could further be tracked by SPT, as illustrated in the right column of Figure 5 which shows the tracks overlaid with the corresponding brightfield image of the cell. The images in Figure 5 were acquired at different time points over 1.5 hours, and further illustrate how liposomes were observed to gradually move in from the edges towards the centre of the cells. No liposomes were observed to enter the space under the cells by diffusion from the surrounding medium. They rather appeared to have already bound to the membrane when they became visible in the field of view. This observation suggests that liposomes do not in fact enter the evanescent field by diffusing between the surface and the cells. It rather appears that liposomes that are not taken up immediately after attaching to the apical membrane move towards the basal membrane, gradually surrounding the cells. These liposomes appear to remain attached to the cell surface without fusing with it.

The tracks in Figure 5 follow liposome movement over the course of 200 seconds. During this short time, the tracks do not reveal any directed inwards movement from the edge towards the cell centre. Such short-scale time-lapses could instead be used to probe the diffusion behaviour of liposomes bound to the cell membrane. Here, two types of movement could be identified among the tracked liposomes. A number of liposomes showed limited movement on the short time-scale: these liposomes appeared more or less stationary and did not exhibit the random movement pattern of freely diffusing particles. One conceivable explanation for liposomes to appear stationary would be that they have attached to the glass surface instead of the cell. This, however, seems unlikely as the functionalized liposomes were, in general, very rarely seen attached to the surface between cells as confirmed by Figure 7. Some liposomes however exhibited a considerable mobility. In this case, the movement appeared to be confined or possibly directed, as seen in Figure 6, independently of whether time lapses were acquired shortly after addition of the liposomes or later on. The overview image provided in Figure 7 further confirms that the results shown for a single cell in Figure 5 are representative for the whole cell population.

In these experiments, no obvious liposome uptake events could be identified. Nevertheless, it is interesting to note that with time, a diffuse increase in the overall fluorescence of cells was

observed (see Figure 5). This observation suggests that uptake might have occurred even though individual liposome uptake events could not be imaged in the time-lapses presented here.

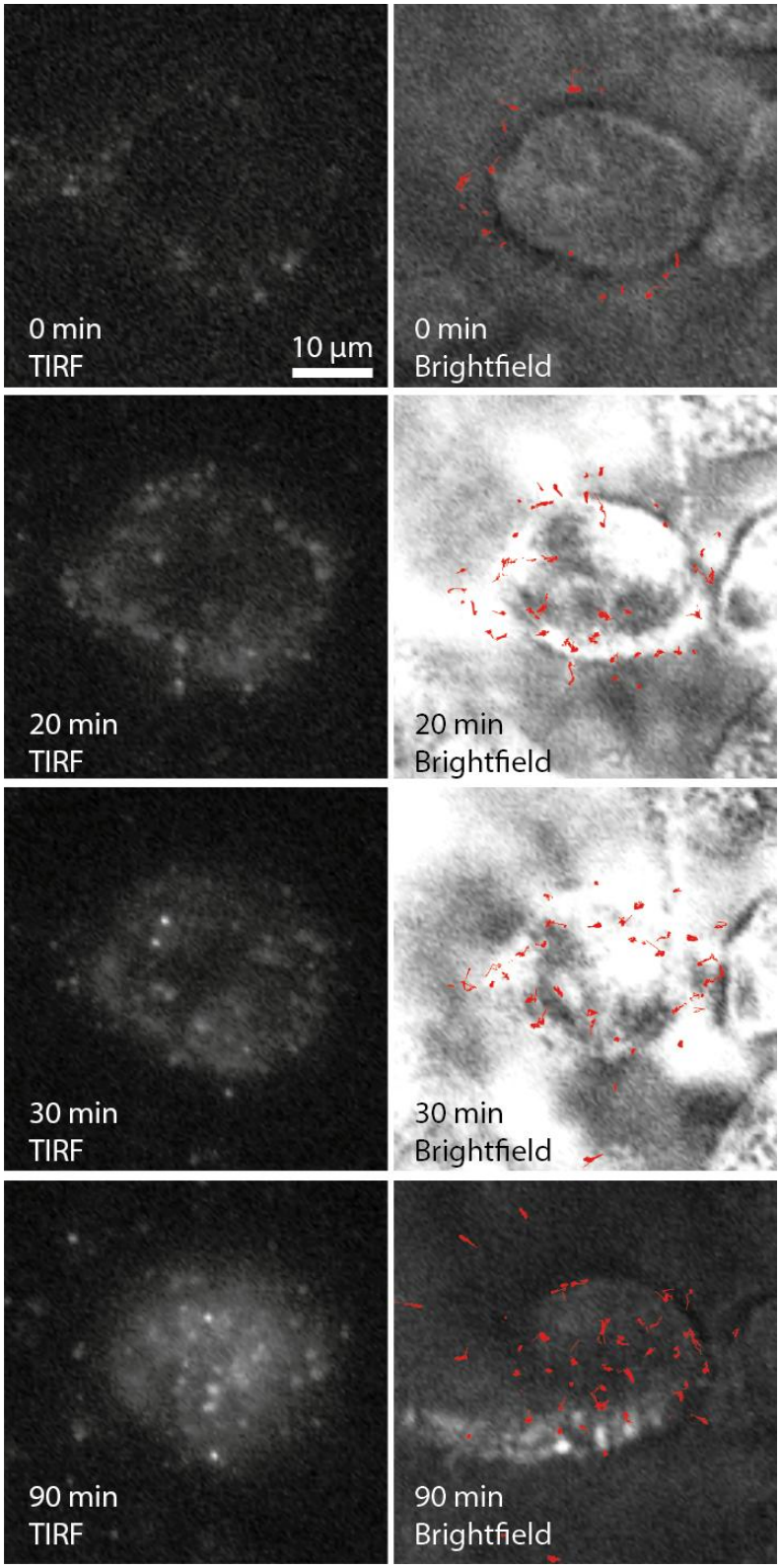

Figure 5. TIRF images in the left column show an IFN-γ-treated FSDC in complete Leibovitz's L15 with Phenol Red at different time points after addition of functionalized liposomes. Images in the right column are the corresponding brightfield images overlaid with the tracks of the liposomes attached to the cell surface.

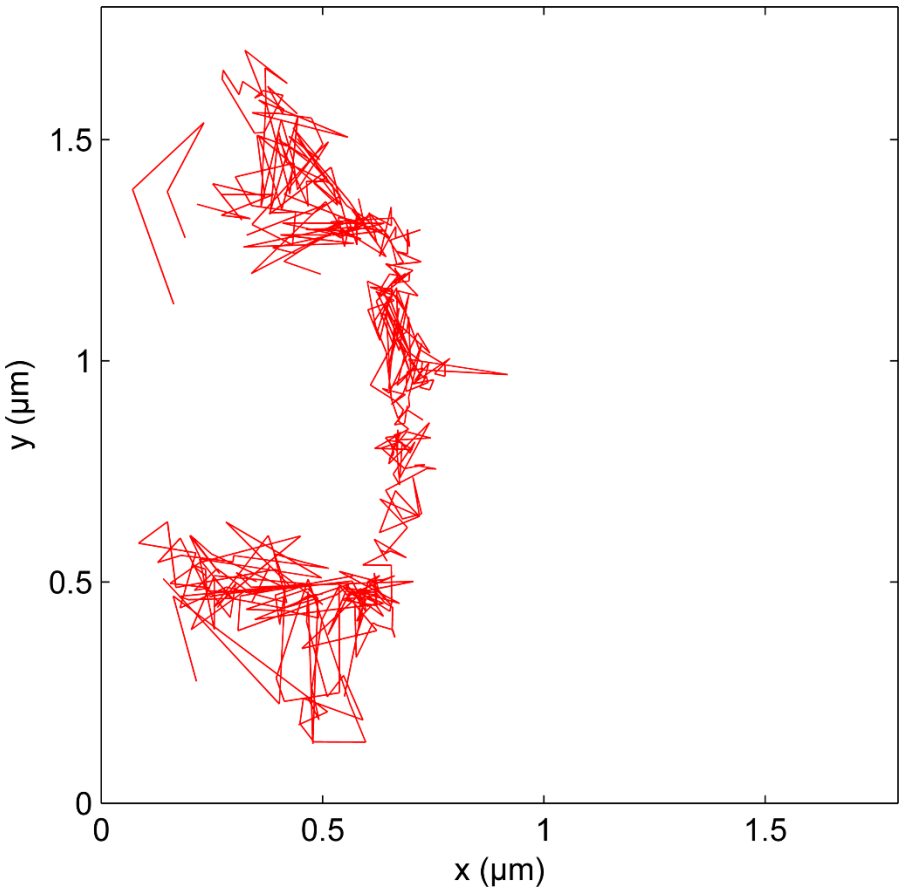

Figure 6. Detail from Figure 5, a magnification of one of the tracks 90 minutes after liposome addition.

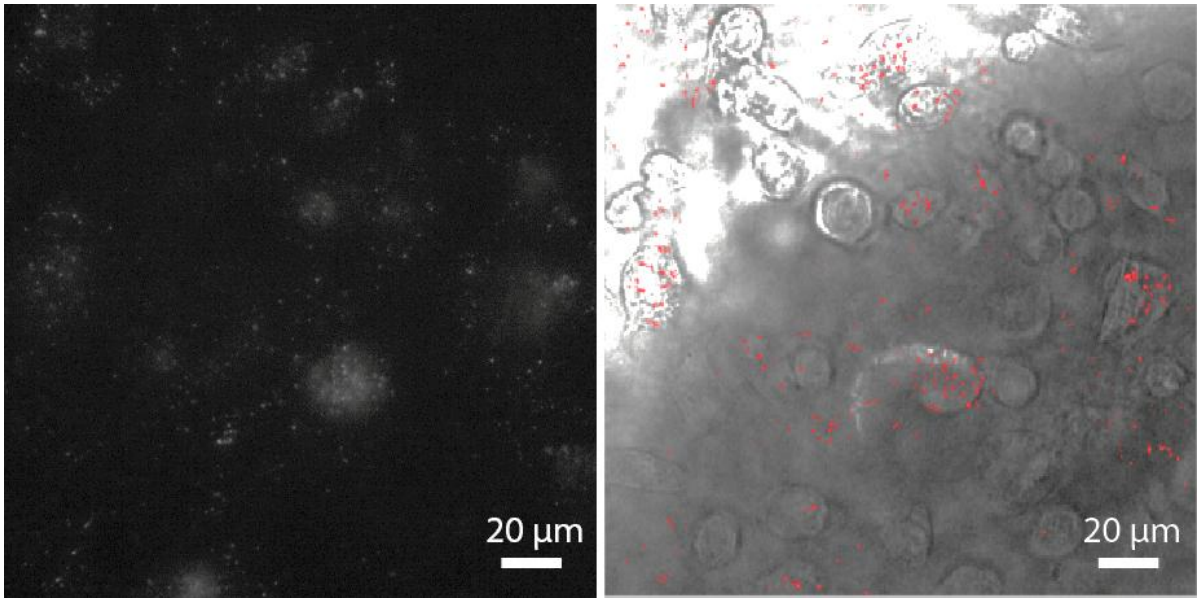

Figure 7. The left image shows functionalized liposomes attached to IFN-γ-treated FSDCs in complete Leibovitz's L15 with Phenol Red, 90 minutes after liposome addition. The right image shows the same view in brightfield overlaid with the tracks of the liposomes attached to the cell surfaces.

6.3 MIXING LIPOSOMES WITH COOLED, DETACHED CELLS

In a second approach, detached cells were incubated with liposomes on ice with the aim of achieving an even distribution of the liposomes on the cell membrane while supressing internalization during incubation [21]. This approach is schematically shown in Figure 2B. A possible advantage of this approach is that it might enable observation earlier in the internalization process compared to what was achieved with the above-mentioned approach, where attached liposomes only slowly progressed into the field of view. The SPT results obtained with this experimental procedure can be seen in Figure 8. Again, the tracks follow the liposome movement over 200 seconds and the results are similar to those obtained with the approach presented in section 6.2; the observed movements of some liposomes are confined while others are to a large extent immobilized. The confined movement can be seen especially well in the magnification shown in Figure 8 and in the trajectory in Figure 9. Furthermore, the typical track length observed using this approach (Figure 9) was on the same order of magnitude as for the approach described in 6.2 (Figure 6).

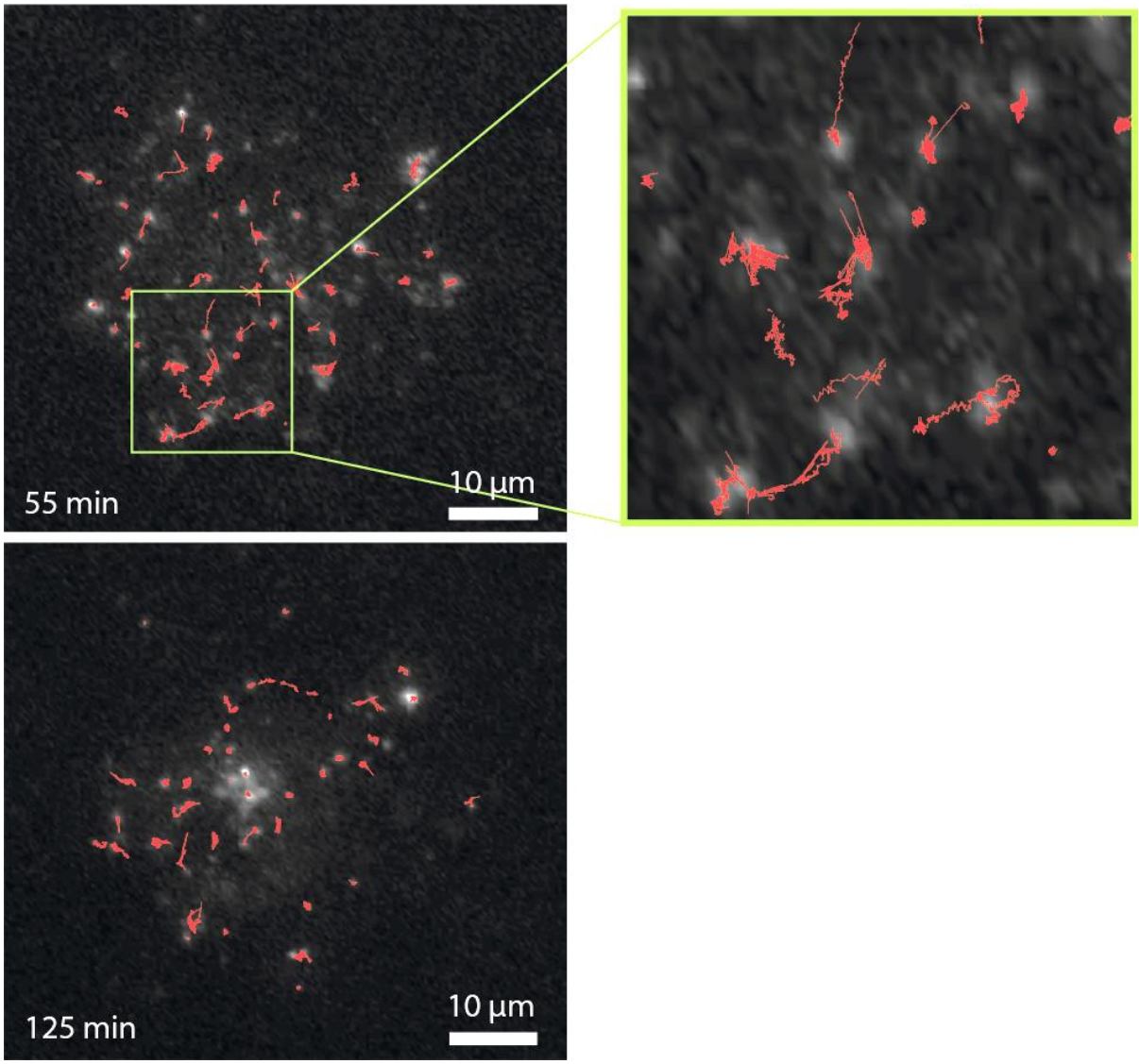

Figure 8. The images show functionalized liposomes attached to IFN-γ-treated FSDCs in complete Leibovitz's L15 with Phenol Red at different time points after starting to warm the sample following incubation on ice. The tracks are overlaid on the corresponding TIRF images.

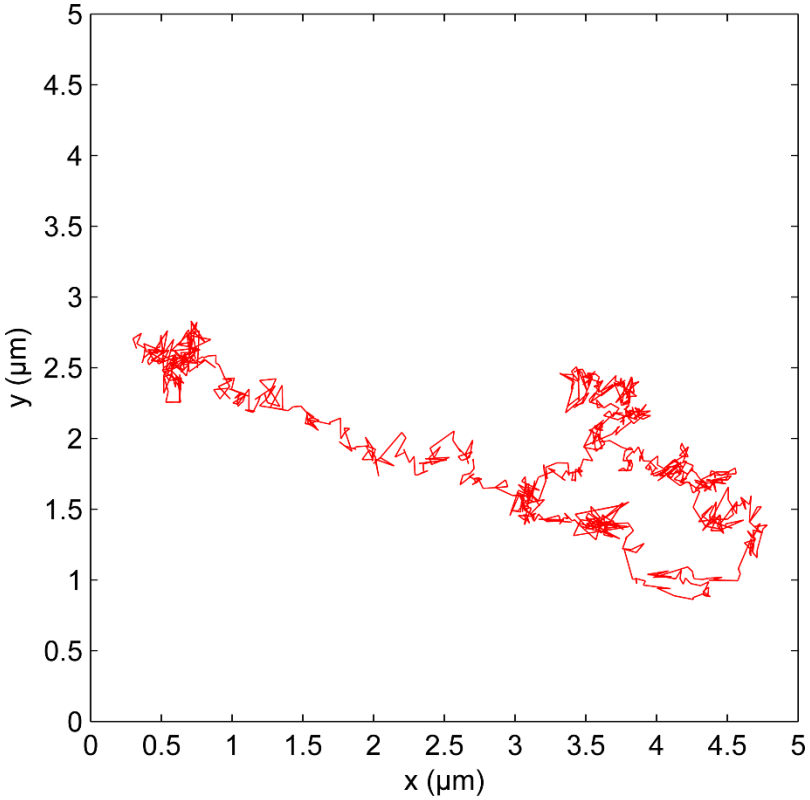

Figure 9. Detail from Figure 8, a magnification of one of the tracks 55 minutes after starting to warm the sample.

To gain further insights into the behaviour of the functionalized liposomes, these results were compared with the ones obtained using positively charged liposomes. These liposomes did not carry the vaccination construct but interacted with the cell surface via electrostatic interactions. Figure 10 shows tracks from such an experiment. In this case, as in the previously presented ones, liposomes were either immobile or showed confined movement. The cationic liposomes bound non-specifically to the glass between the cells to a larger extent than the functionalized ones but only the cell-bound liposomes exhibited any mobility.

Since uptake events could be identified neither in the time-lapses presented in section 6.2 nor in this section, where data from both functionalized and positively charged liposomes has been presented, the question whether liposome uptake by the FSDCs actually occurred is raised.

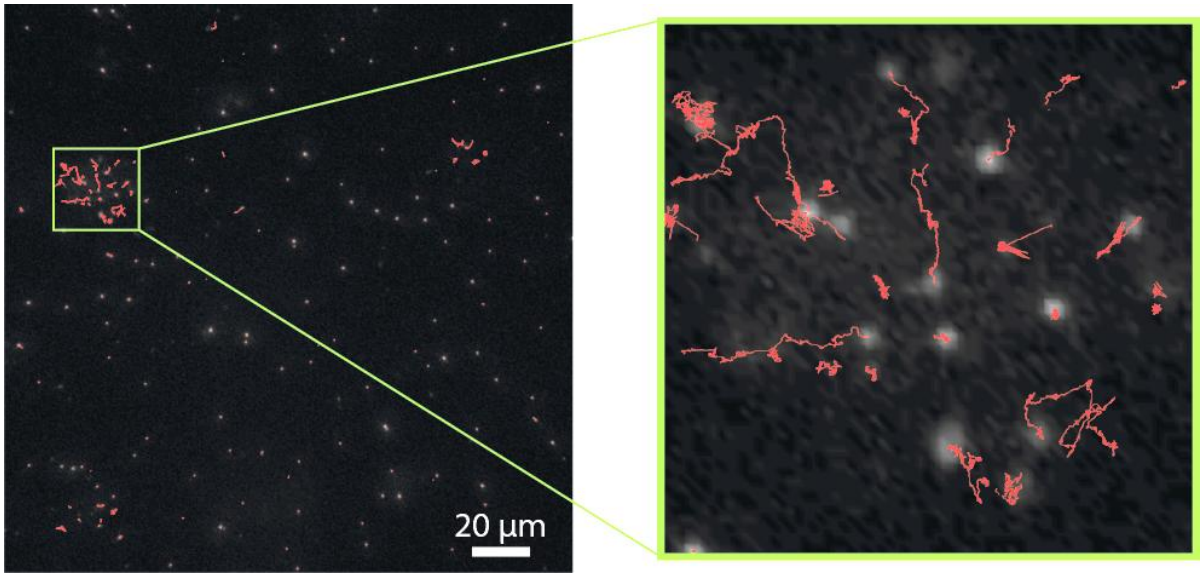

Figure 10. The images show tracks of single positive liposomes on the surfaces of FSDCs in complete IMDM with Phenol Red, overlaid on the corresponding TIRF image. The time-lapse was taken 13 minutes after initiation of sample heating after incubation on ice. The image on the right shows a magnification of the cell marked with a green square in the left image.

In addition to this, it is important to stress that, even though SPT could be performed on some cells, for the approach presented in this section, only a very small number of cells could be visualized by TIRF microscopy. This is illustrated in the overview image in Figure 11 where, additionally, it is visible that the cells had to display a certain, flattened morphology (Figure 11, right) in order to come close enough to the surface to appear in the field of TIR illumination. This morphology is different from what is regularly seen in this cell type which raises the question of whether these cells are representative or if the data collected is skewed. Another drawback uncovered during these experiments was that the microincubator used for heating the samples was unable to reach temperatures higher than 28°C. This is most likely due to the fact that an open system was used and that the objective acted as a heat sink, constantly cooling the sample. That the temperature did not reach physiological levels might have further affected the behaviour of the cells in these experiments and might be related to the unusual morphology that was observed.

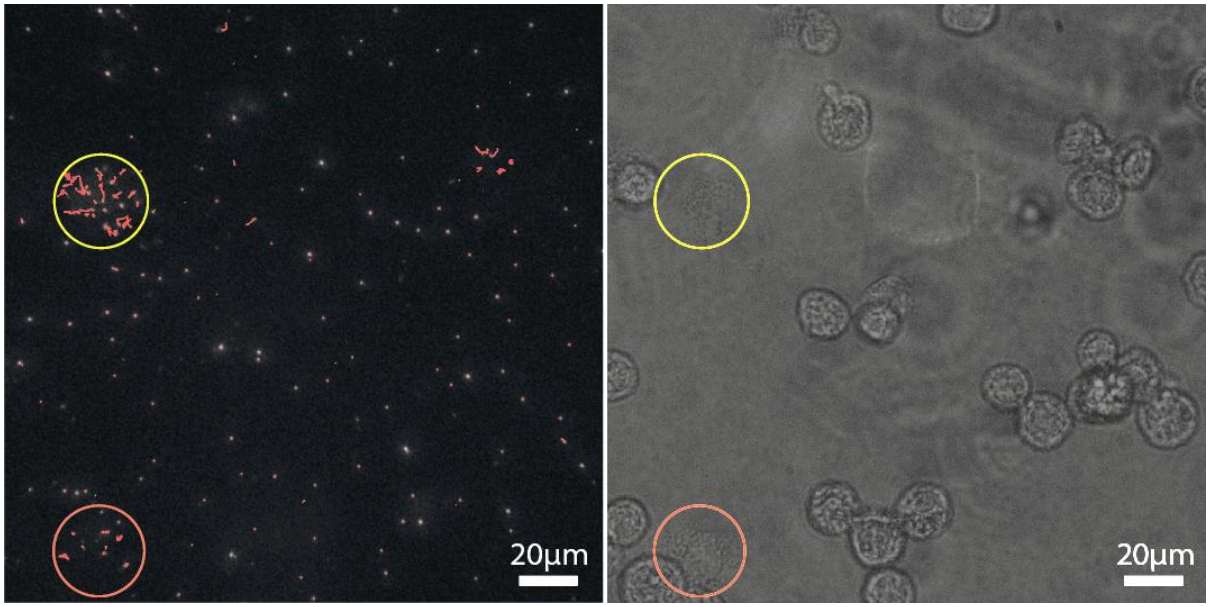

Figure 11. Images show FSDCs incubated with positive liposomes on ice, in complete IMDM with Phenol Red. The left image shows the cells in TIR illumination and the right image in brightfield.

6.4 Addition of Liposomes to Cooled, Adhered Cells

The approaches presented so far have been proven useful in characterizing particle movement at the cell surface. However, individual particle uptake events could not be confirmed. To provide an alternative way of quantifying uptake, we investigated whether it is possible to quantify the decrease in number of intact liposomes present at the membrane of the cell, or in the cell after internalization. In the approach schematically shown in Figure 2C, surface-attached cells were incubated with liposomes on ice in order to ensure attachment of the carriers while delaying uptake. Excess liposomes in solution were removed by rinsing prior to heating and imaging to ensure that no additional liposomes attached to the cell membrane once imaging had started. Epifluorescence microscopy, which has a deeper field of illumination than TIRF, was used. In order to capture as much as possible of the cell while excluding any liposomes that may be immobilized at the glass surface, the images were taken slightly above the glass surface. While epifluorescence microscopy did indeed give a deeper field of illumination, the focus was still limited to a thin section of the cell with liposomes situated beyond this plane appearing blurry, making accurate quantification problematic. Figure 12 displays the total number of vesicles attached to the cell over time. As visible, there was no clear decrease in number of attached liposomes and the approach could not be used to quantify uptake without further development. Furthermore, only few liposomes were detected on the cells, possibly since IFN-γ, a cytokine that increases the endocytic activity of dendritic cells, was not used in this experiment. Another possible explanation is liposome aggregation. During the course of the project it was in fact observed that liposomes carrying the vaccine construct became inactive with time and it was

suspected that aggregation was the cause. It is however unclear how fast such a process might occur. Aggregation might also explain the fact that, using this approach, it was not possible to observe functionalized liposomes using TIRF microscopy, as shown in Figure 13. It was however possible to visualise the positively charged liposomes in TIRF which indicates that the functionalized liposomes were not as easily transported to the underside of the cells as the positive ones. This may however also be ascribed to a difference in size resulting from the fact that a membrane with larger pore size was used in the production of the functionalized liposomes than in the production of the positive ones.

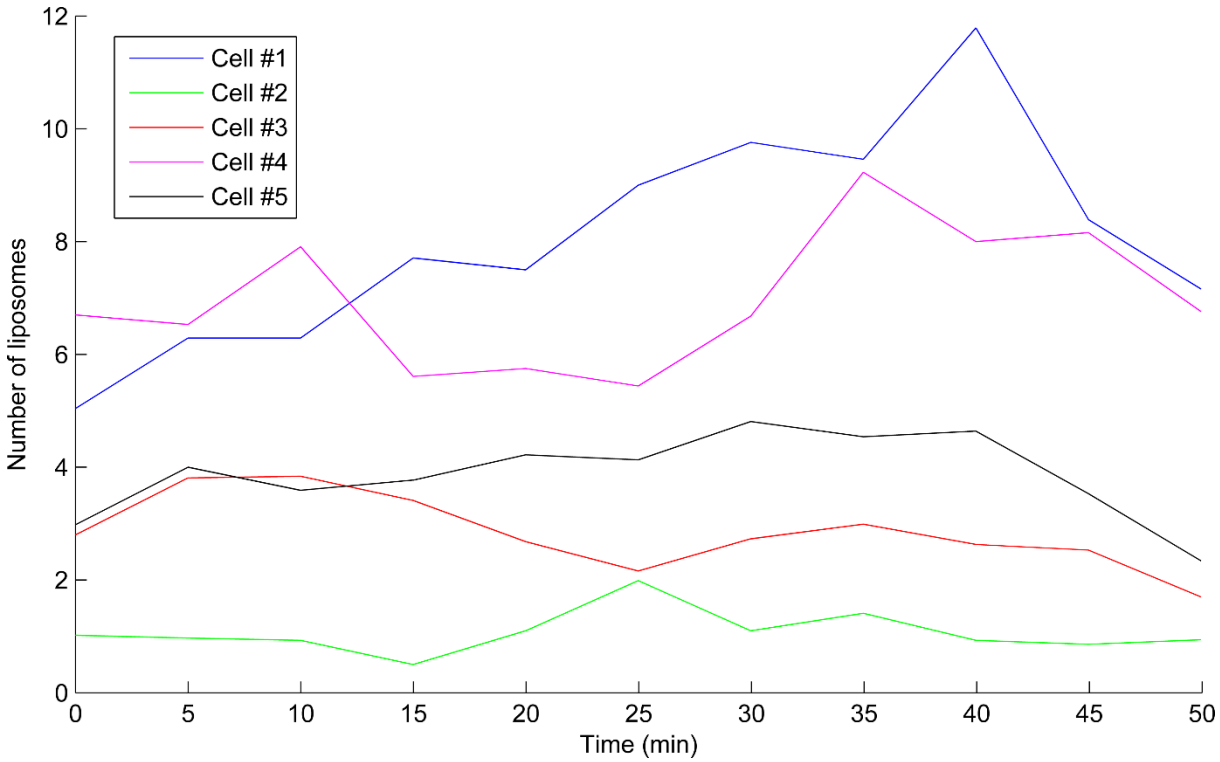

Figure 12. Number of attached functionalized liposomes to the surface of attached, cooled FSDCs. The images analyzed to obtain this data was taken just above the surface.

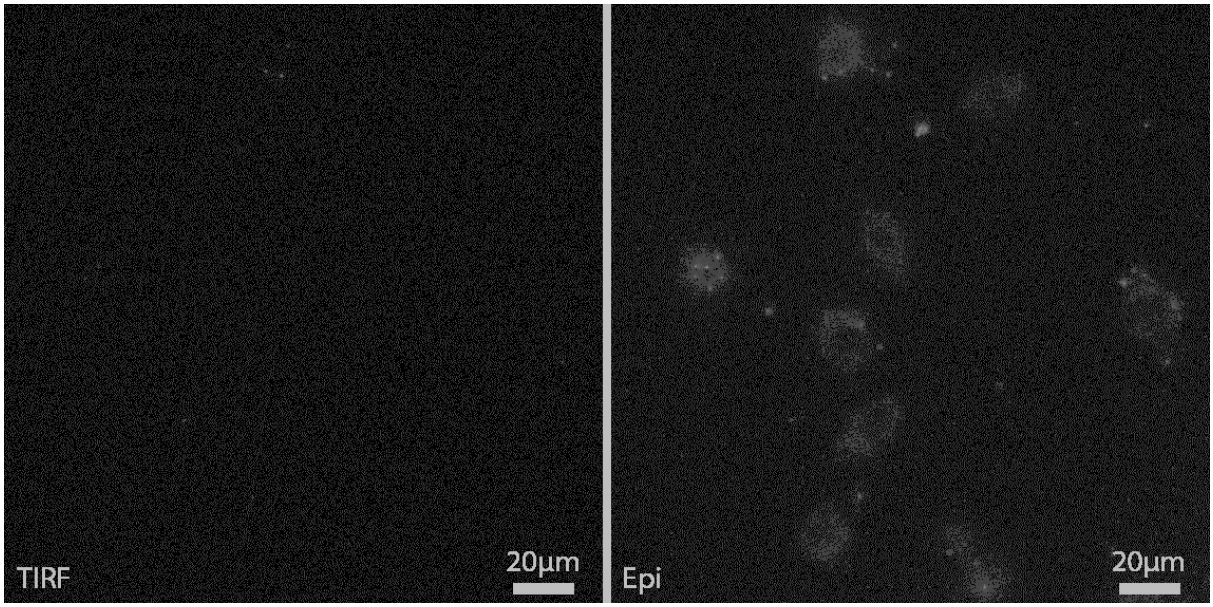

Figure 13. Images show adhered FSDCs incubated on ice with functionalized liposomes, in Leibovitz's L15 without serum and Phenol Red. The images were taken at the surface.

In conclusion, there is still some development required before this approach works as intended. The use of a lower-magnification objective might extend the depth of the focus plane. Alterations to the rinsing procedure might change the outcome of the approach which is based on the assumption that no additional liposomes can attach to the cell during imaging. Furthermore, it is worth noting that in Figure 13, the cells can be seen to have a weak autofluorescence that was present before addition of the liposomes, indicating that uptake of other material could have occurred prior to imaging.

7 DISCUSSION

7.1 INITIAL ATTACHMENT OF LIPOSOMES TO CELLS

SPT enables monitoring and characterization of the various steps of uptake processes and can help identify ways of improving a certain carrier formulation in order to streamline the uptake [47]. In order to accurately identify distinct features of a particular uptake event and allow for comparison between different particle formulations, it is necessary to have a common reference point. The point of initial attachment is a feature that recurs for all particles and could be used for this purpose. Furthermore, the kinetics of particle-cell binding is of particular interest as the initial attachment may be the controlling and limiting step in the uptake process. For this reason, Chenevier *et al.* [48] and Lee *et al*. [49] studied the adhesion process of liposomes to cells and determined the binding rate constant. Our work aspired to characterize liposomal attachment to cells in a similar manner. However, in the approach with adhered cells (section 6.2), it was not possible for the liposomes to diffuse between the cell membrane and the surface. The initial attachment to the basal membrane was thus not observed. Instead, the liposomes appeared to attach to the apical membrane to later slowly be transported to the underside of the cells. In the approach with cooled, detached cells (section 6.3), observation of the initial attachment was not expected, since the liposomes had already attached prior to imaging.

7.2 MOVEMENT OF CELL-BOUND LIPOSOMES

It is of interest to be able to characterize the movement of liposomes on the cell surface as little is known about the influence different liposome formulations have on this process. Generally speaking, movement of particles on the cell surface can provide important clues about the nature of the interaction between the particles and the membrane. For example, in the study of Sindbis virion-cell surface binding, two movement types were identified, indicating the incidence of two separate types of receptor-virus interactions [50]. Identification and characterization of distinct stages of movement of influenza virions on the cell surface was used by Rust *et al.* [51] in order to determine when internalization had occurred and in extension to elucidate the internalization pathways. De Bruin *et al.* [18] used a similar strategy in the study of EGF polyplex uptake and were able to distinguish different modes of endocytosis by the difference in duration of a certain movement phase. In a study by Aaron *et al.* [21] it was shown that the size and shape of quantum dots influence both their final intracellular fate and their behaviour on the cell membrane; more specifically, quantum dots with a high aspect ratio exhibited slower movement. In a similar manner, it would be interesting to clarify whether different liposomal vaccine formulations would cause differences in movement behaviour and whether this could be correlated to vaccine

efficacy. The establishment of reliable methods are necessary to enable such research and in this work, TIRF microscopy has been shown to be a useful tool to acquire good quality images, suitable for SPT analysis.

In both approaches described in sections 6.2 and 6.3, liposomes were found to either be immobilized or to exhibit confined, possibly directed, movement. Similar liposome behaviour was observed irrespective of the time point, how the sample was prepared and which liposome type was used. This indicates that the observed movement behaviour is neither an artefact due to sample handling nor a behaviour specific to the functionalized liposomes. It was concluded that the stationary liposomes were not likely attached to the glass surface but rather to the cell membrane. Immobile cell-bound particles have been observed by others; for example by Gu *et al*. [50] who observed immobile cell-bound Sindbis virions and concluded that this behaviour was likely due to nonspecific particle-receptor binding, something that might apply also in this case. It appears that 200 seconds might not be long enough for these cells to exhibit considerable movement since the immobile liposomes do not shift over the course of the time-lapses. Similarly, the confined movement observed in the other subpopulation of the liposomes is unlikely to be the a result of the cell moving on the surface as liposome movement is neither coordinated in one direction as if the cell was migrating, nor outward as if the cell was spreading. It could instead possibly be explained by the morphology of dendritic cells, whose antennae-like dendrites become more skirt-like upon activation [52]. It is thus conceivable that the FSDCs are activated and that the confined movement of the liposomes takes place along the ridge of such protrusions on the cell surfaces. Activation of the FSDCs could be triggered by the liposomes themselves or by something else, prior to addition of the liposomes.

7.3 Liposome Uptake in Cells

The kinetics of cellular uptake of liposomes has previously been studied in order to utilize the understanding of the governing mechanisms to improve the design of liposomal carrier systems [49, 53, 54]. Furthermore, particle uptake by cells has been studied with the ambition of assessing the efficiency of different targeting strategies for various delivery applications [18, 53]. Similarly, the nature of the possible correlation between the number, mode and/or speed of uptake of vaccination liposomes by dendritic cells with the successful induction of a strong immune response could be useful information for the future development of vaccines. In fact, it is especially interesting since antigen uptake by dendritic cells is crucial to induce a primary immune response [25].

Studying individual particles allows for a very high temporal resolution of the uptake process [18] and can be applied to study the very moment that uptake occurs [16, 19]. Generally speaking,

liposome uptake is likely to occur via two processes; the liposome can be taken up via endocytosis or by fusing with the lipid membrane. The first scenario would result in a sudden disappearance of the liposome, possibly together with a diffuse spreading of the fluorescence as the liposome moves out of focus. In the second case, the disappearance of an individual liposome is followed by a localized increase of fluorescence in the cell membrane, characteristic for a fusion process. This type of uptake is described by van der Schaar *et al*. [16] and Schmidt *et al*. [19] but was not detectable in any of the time-lapses acquired in this work. The detection of endocytosis proved to be challenging as liposomes were observed to suddenly appear under cells, seemingly from above, and liposomes that had disappeared out of view would appear to return again. This observation might be explained by the changes in dendritic cell morphology that takes place upon activation as described in section 7.2. If the dendritic cells were activated during imaging it is possible that the liposomes were in fact moving in and out of the field of TIR illumination, between the cell protrusions. The fact that liposomes could leave the evanescent field under a cell, without being taken up, meant that individual uptake events via endocytosis could neither be ascertained nor excluded. Furthermore, it is possible that the experimental time window did not allow for visualization of individual uptake events, and in particular that such events occurred before acquisition of the time-lapses, considering the previously mentioned possible changes in cell morphology. This would be particularly problematic as dendritic cells cease to actively take up antigens upon activation and instead proceed to activate other immune cells by presenting them with antigens [26]. An indication in line with the hypothesis that the cells have already taken up fluorescent material prior to the experiments is the faint autofluorescence that can be observed in the cells in Figure 13.

Results that indicate that uptake does, in fact, occur during the experimental time window, is the increase in the diffuse background fluorescence of cells that was observed over time, as visible in Figure 5. The overall fluorescence increase could be associated with incorporation of fluorescent lipids into the cell membrane due to fusion between liposomes and the cell membrane. It could also possibly reflect an accumulation of liposomes close to the cell membrane, within the cell, caused by endocytosis. It is unlikely that it was caused by an increased background from accumulation of liposomes on the apical membrane due to the limited field of view given by the TIR illumination. That the overall increase in fluorescence with time seen in Figure 5 was not as prominent in the approaches where cells were cooled might be ascribed to the problems with controlling the temperature that recurred in all approaches. These problems were especially noticeable in the two approaches where the samples were cooled and were likely affecting the endocytic activity of the cells. In fact, the results in Figure 11 bring into question how much the cells were affected by the cooling and subsequent slow heating. The unusual cell morphology

observed there might be in response to this or due to the cells being activated by the liposomes. A fact that speaks against the latter is that the same is not seen in the approach described in section 6.2, where the cells were not cooled. It would be necessary to examine if the cooling process affects the viability of the cells. It is possible that with a more effective approach to heating the system, the results would have been different.

In conclusion, further experiments are needed to assess whether or not liposomes are being taken up by the FSDCs. Confocal microscopy on cells with a cytosolic stain or with labelled endocytic vesicles could be used to ascertain whether liposomes are present within the cells, providing some indication of whether endocytosis has occurred. Cy3-labelled liposomes and selective quenching of the extracellular ones with Trypan Blue could be used to the same end with possible additional quantification of the amount of endocytosed liposomes. Finally, fluorescence recovery after photobleaching (FRAP) experiments are likely to provide further insights into the mechanism of uptake as they can provide information on whether labelled lipids are present in the cell membrane or if the liposomes are accumulated within the cell or on the membrane, slightly above the level of focus, so that they appear blurry.

Another factor worth investigating in a more systematic manner, is the influence of the liposome size on the assay performance. It is intriguing that the functionalized liposomes were not visible in TIRF (Figure 13) during the experiments with adhered, cooled cells while positive liposomes were, during preliminary experiments. The cooling of the cells causes rigidity of the membrane which is likely prolonged due to the slow heating. This might reduce the likelihood for the larger liposomes to be accommodated in the limited space between the membrane and the surface, explaining how the functionalized liposomes could pass under the cells in the approach in section 6.2, but not in the one in section 6.4.

8 CONCLUSION AND OUTLOOK

In this work, it was proved possible to visualize liposomes attached to the basal membrane of FSDCs. Furthermore, SPT could be performed both in the approach with adhered cells and in the approach with cooled, detached cells (sections 6.2 and 6.3). The SPT results revealed that liposomes were, to a large extent, immobilized on the cell surface and the observed movement was mainly confined in nature.

Despite promising results with SPT, we were unable to capture the initial attachment of liposomes. In the approach with adhered cells, the liposomes did not diffuse under the cells to subsequently attach to the membrane but instead attached to the apical membrane and slowly moved into the field of view at the basal membrane. In the approach with cooled, detached cells, it proved difficult to capture the descent of cells towards the surface. Few cells came close enough to the surface to be imaged and those who did displayed an unusual morphology which raised concerns about the cells being adversely affected by the cooling and/or slow and incomplete return to physiological temperature.

There is not yet a finalized method for quantifying particle uptake since the approach with cooling attached cells and quantifying the attached liposomes (section 6.4) does not work to date. This approach still has possibilities for development: the rinsing needs to be optimized as there were clearly still liposomes present in solution.

There are a few other modifications to the set-up and additional experiments that need to be performed before more drastic changes to the system are implemented. Firstly, since heating with the stage microincubator proved to be insufficient, the temperature control needs to be improved to ensure the validity of future work. It is also possible that more effective heating might change the outcomes of some of the experiments described here. An objective heater might be sufficient as it would prevent the objective from acting as a heat sink.

An interesting possible extension of this project, if the suggested improvements to the system are ineffective, would be to develop alternative approaches that facilitate liposome diffusion between cell membrane and substrate. One such approach could be the use of a topographically patterned surface with pillars intended to act as spacers as schematically shown in Figure 14. Another possibility would be to grow cells on top of a functional surface capable of triggering liposome release upon an external stimuli. Such a functionalization could be created by coupling DNA oligomers to a surface and anchoring liposomes using slightly mismatched DNA strands. The liposomes could then be released by adding DNA strands that are fully complementary to the ones coupled to the surface. Another possibility would be to use a thermosensitive polymer such as

poly(N-isopropylacrylamide) in a manner similar to what has previously been done to achieve controlled drug release [55].

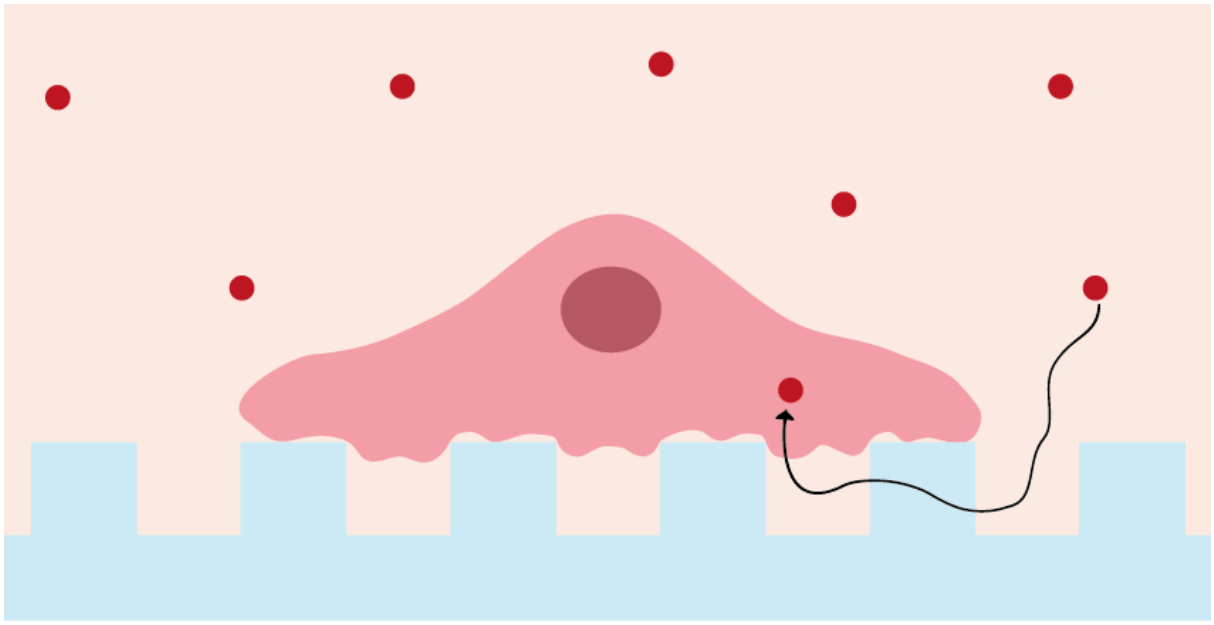

Figure 14. A schematic image of an approach with a topographically patterned surface with pillars to allow diffusion of liposomes between the cells and the surface.

In conclusion, we have taken the first step on the road towards an assay for the study of uptake of functionalized liposomes by dendritic cells. There is still plenty of work to do, both in developing the assay and in characterizing the liposomes in order to gain knowledge about the carrier system we are attempting to study.

9 REFERENCES

[1] T. M. Allen and P. R. Cullis, "Drug delivery systems: Entering the mainstream," *Science,* vol. 303, pp. 1818-1822, Mar 2004.

[2] L. J. Peek, C. R. Middaugh, and C. Berkland, "Nanotechnology in vaccine delivery," *Advanced Drug Delivery Reviews,* vol. 60, pp. 915-928, May 2008.

[3] A. D. Bangham, M. M. Standish, and J. C. Watkins, "Diffusion of univalent ions across lamellae of swollen phospholipids," *Journal of Molecular Biology,* vol. 13, pp. 238-252, 1965.

[4] G. Gregoriadis, E. J. Wills, C. P. Swain, and A. S. Tavill, "Drug-carrier potential of liposomes in cancer chemotherapy," *Lancet,* vol. 1, pp. 1313-1316, 1974.

[5] V. P. Torchilin, "Recent advances with liposomes as pharmaceutical carriers," *Nature Reviews Drug Discovery,* vol. 4, pp. 145-160, Feb 2005.

[6] A. K. Giddam, M. Zaman, M. Skwarczynski, and I. Toth, "Liposome-based delivery system for vaccine candidates: constructing an effective formulation," *Nanomedicine,* vol. 7, pp. 1877-1893, Dec 2012.

[7] D. S. Watson, A. N. Endsley, and L. Huang, "Design considerations for liposomal vaccines: Influence of formulation parameters on antibody and cell-mediated immune responses to liposome associated antigens," *Vaccine,* vol. 30, pp. 2256-2272, Mar 2012.

[8] S. Merler and M. Ajelli, "The role of population heterogeneity and human mobility in the spread of pandemic influenza," *Proceedings of the Royal Society B-Biological Sciences,* vol. 277, pp. 557-565, Feb 2010.

[9] V. Colizza, A. Barrat, M. Barthelemy, and A. Vespignani, "The role of the airline transportation network in the prediction and predictability of global epidemics," *Proceedings of the National Academy of Sciences of the United States of America,* vol. 103, pp. 2015-2020, Feb 2006.

[10] N. Lycke, "Recent progress in mucosal vaccine development: potential and limitations," *Nature Reviews Immunology,* vol. 12, pp. 592-605, Aug 2012.

[11] S. Chadwick, C. Kriegel, and M. Amiji, "Nanotechnology solutions for mucosal immunization," *Advanced Drug Delivery Reviews,* vol. 62, pp. 394-407, Mar 2010.

[12] D. G. Eliasson, K. El Bakkouri, K. Schoen, A. Ramne, E. Festjens, B. Lowenadler*, et al.*, "CTA1-M2e-DD: A novel mucosal adjuvant targeted influenza vaccine," *Vaccine,* vol. 26, pp. 1243-1252, Feb 2008.

[13] Y. F. Ma, Y. Zhuang, X. F. Xie, C. Wang, F. Wang, D. M. Zhou*, et al.*, "The role of surface charge density in cationic liposome-promoted dendritic cell maturation and vaccine-induced immune responses," *Nanoscale,* vol. 3, pp. 2307-2314, 2011.

[14] L. Parhamifar and S. M. Moghimi, "Total internal reflection fluorescence (TIRF) microscopy for real-time imaging of nanoparticle-cell plasma membrane interaction," *Methods in molecular biology (Clifton, N.J.),* vol. 906, pp. 473-82, 2012 2012.

[15] A. L. Mattheyses, S. M. Simon, and J. Z. Rappoport, "Imaging with total internal reflection fluorescence microscopy for the cell biologist," *Journal of Cell Science,* vol. 123, pp. 3621-3628, Nov 2010.

[16] H. M. van der Schaar, M. J. Rust, C. Chen, H. van der Ende-Metselaar, J. Wilschut, X. W. Zhuang*, et al.*, "Dissecting the Cell Entry Pathway of Dengue Virus by Single-Particle Tracking in Living Cells," *Plos Pathogens,* vol. 4, p. 9, Dec 2008.

[17] L.-W. Chu, Y.-L. Huang, J.-H. Lee, L.-Y. Huang, W.-J. Chen, Y.-H. Lin*, et al.*, "Single-virus tracking approach to reveal the interaction of Dengue virus with autophagy during the early stage of infection," *Journal of biomedical optics,* vol. 19, p. 011018, 2014 2014.

[18] K. de Bruin, N. Ruthardt, K. von Gersdorff, R. Bausinger, E. Wagner, M. Ogris*, et al.*, "Cellular dynamics of EGF receptor-targeted synthetic viruses," *Molecular Therapy,* vol. 15, pp. 1297-1305, Jul 2007.

[19] F. I. Schmidt, P. Kuhn, T. Robinson, J. Mercer, and P. S. Dittrich, "Single-Virus Fusion Experiments Reveal Proton Influx into Vaccinia Virions and Hemifusion Lag Times," *Biophysical Journal,* vol. 105, pp. 420-431, Jul 2013.
[20] H. Jin, D. A. Heller, R. Sharma, and M. S. Strano, "Size-Dependent Cellular Uptake and Expulsion of Single-Walled Carbon Nanotubes: Single Particle Tracking and a Generic Uptake Model for Nanoparticles," *Acs Nano,* vol. 3, pp. 149-158, Jan 2009.
[21] J. S. Aaron, A. C. Greene, P. G. Kotula, G. D. Bachand, and J. A. Timlin, "Advanced Optical Imaging Reveals the Dependence of Particle Geometry on Interactions Between CdSe Quantum Dots and Immune Cells," *Small,* vol. 7, pp. 334-341, Feb 2011.
[22] A. L. Mattheyses, C. E. Atkinson, and S. M. Simon, "Imaging Single Endocytic Events Reveals Diversity in Clathrin, Dynamin and Vesicle Dynamics," *Traffic,* vol. 12, pp. 1394-1406, Oct 2011.
[23] T. Tian, Y. L. Zhu, F. H. Hu, Y. Y. Wang, N. P. Huang, and Z. D. Xiao, "Dynamics of exosome internalization and trafficking," *Journal of Cellular Physiology,* vol. 228, pp. 1487-1495, Jul 2013.
[24] B. Pulendran and R. Ahmed, "Immunological mechanisms of vaccination," *Nature Immunology,* vol. 12, pp. 509-517, Jun 2011.
[25] J. Banchereau, F. Briere, C. Caux, J. Davoust, S. Lebecque, Y. T. Liu*, et al.*, "Immunobiology of dendritic cells," *Annual Review of Immunology,* vol. 18, pp. 767-+, 2000 2000.
[26] J. Banchereau and R. M. Steinman, "Dendritic cells and the control of immunity," *Nature,* vol. 392, pp. 245-252, Mar 1998.
[27] J. E. McElhaney, D. X. Xie, W. D. Hager, M. B. Barry, Y. Z. Wang, A. Kleppinger*, et al.*, "T cell responses are better correlates of vaccine protection in the elderly," *Journal of Immunology,* vol. 176, pp. 6333-6339, May 2006.
[28] J. Wang, L. Thorson, R. W. Stokes, M. Santosuosso, K. Huygen, A. Zganiacz*, et al.*, "Single mucosal, but not parenteral, immunization with recombinantadenoviral-based vaccine provides potent protection from pulmonary tuberculosis," *Journal of Immunology,* vol. 173, pp. 6357-6365, 2004.
[29] A. des Rieux, V. Fievez, M. Garinot, Y. J. Schneider, and V. Preat, "Nanoparticles as potential oral delivery systems of proteins and vaccines: A mechanistic approach," *Journal of Controlled Release,* vol. 116, pp. 1-27, Nov 2006.
[30] J. L. Owen, B. Sahay, and M. Mohamadzadeh, "New generation of oral mucosal vaccines targeting dendritic cells," *Current opinion in chemical biology,* vol. 17, pp. 918-24, 2013.
[31] S. T. Reddy, M. A. Swartz, and J. A. Hubbell, "Targeting dendritic cells with biomaterials: developing the next generation of vaccines," *Trends in Immunology,* vol. 27, pp. 573-579, Dec 2006.
[32] M. Prato, K. Kostarelos, and A. Bianco, "Functionalized carbon nanotubes in drug design and discovery," *Accounts of Chemical Research,* vol. 41, pp. 60-68, Jan 2008.
[33] T. Lian and R. J. Y. Ho, "Trends and developments in liposome drug delivery systems," *Journal of Pharmaceutical Sciences,* vol. 90, pp. 667-680, Jun 2001.
[34] L. Illum, I. Jabbal-Gill, M. Hinchcliffe, A. N. Fisher, and S. S. Davis, "Chitosan as a novel nasal delivery system for vaccines," *Advanced Drug Delivery Reviews,* vol. 51, pp. 81-96, Sep 2001.
[35] A. Vila, A. Sanchez, M. Tobio, P. Calvo, and M. J. Alonso, "Design of biodegradable particles for protein delivery," *Journal of Controlled Release,* vol. 78, pp. 15-24, Jan 2002.
[36] B. Gupta, T. S. Levchenko, and V. P. Torchilin, "Intracellular delivery of large molecules and small particles by cell-penetrating proteins and peptides," *Advanced Drug Delivery Reviews,* vol. 57, pp. 637-651, Feb 2005.
[37] L. Josephson, C. H. Tung, A. Moore, and R. Weissleder, "High-efficiency intracellular magnetic labeling with novel superparamagnetic-tat peptide conjugates," *Bioconjugate Chemistry,* vol. 10, pp. 186-191, Mar-Apr 1999.
[38] T. Horimoto and Y. Kawaoka, "Influenza: Lessons from past pandemics, warnings from current incidents," *Nature Reviews Microbiology,* vol. 3, pp. 591-600, Aug 2005.

[39] R. G. Webster, W. J. Bean, O. T. Gorman, T. M. Chambers, and Y. Kawaoka, "Evolution and ecology of Influenza-A viruses," *Microbiological Reviews,* vol. 56, pp. 152-179, Mar 1992.
[40] E. Ghedin, A. Fitch, A. Boyne, S. Griesemer, J. DePasse, J. Bera*, et al.*, "Mixed Infection and the Genesis of Influenza Virus Diversity," *Journal of Virology,* vol. 83, pp. 8832-8841, Sep 2009.
[41] World Health Organization WHO factsheet 211: influenza, 2014.
[42] F. Carrat and A. Flahault, "Influenza vaccine: The challenge of antigenic drift," *Vaccine,* vol. 25, pp. 6852-6862, Sep 2007.
[43] M. P. Girard, J. S. Tam, O. M. Assossou, and M. P. Kieny, "The 2009 A (H1N1) influenza virus pandemic: A review," *Vaccine,* vol. 28, pp. 4895-4902, Jul 2010.
[44] C. Gerdil, "The annual production cycle for influenza vaccine," *Vaccine,* vol. 21, pp. 1776-1779, May 2003.
[45] L. C. Agren, L. Ekman, B. Lowenadler, and N. Y. Lycke, "Genetically engineered nontoxic vaccine adjuvant that combines B cell targeting with immunomodulation by cholera toxin A1 subunit," *Journal of Immunology,* vol. 158, pp. 3936-3946, Apr 1997.
[46] G. Girolomoni, M. B. Lutz, S. Pastore, C. U. Abmann, A. Cavani, and P. Ricciardicastagnoli, "Establishment of a Cell-line with Features of Early Dendritic Cell Precursors from Fetal Mouse Skin," *European Journal of Immunology,* vol. 25, pp. 2163-2169, Aug 1995.
[47] N. Ruthardt, D. C. Lamb, and C. Brauchle, "Single-particle Tracking as a Quantitative Microscopy-based Approach to Unravel Cell Entry Mechanisms of Viruses and Pharmaceutical Nanoparticles," *Molecular Therapy,* vol. 19, pp. 1199-1211, Jul 2011.
[48] P. Chenevier, B. Veyret, D. Roux, and N. Henry-Toulme, "Interaction of cationic colloids at the surface of J774 cells: A kinetic analysis," *Biophysical Journal,* vol. 79, pp. 1298-1309, Sep 2000.
[49] K. D. Lee, S. Nir, and D. Papahadjopoulos, "Quantitative analysis of liposome-cell interactions in vitro - rate constants of binding and endocytosis with suspension and adherent J774-cells and human monocytes," *Biochemistry,* vol. 32, pp. 889-899, Jan 1993.
[50] Y. Gu, Y. Yang, and Y. Liu, "Imaging early steps of sindbis virus infection by total internal reflection fluorescence microscopy," *Advances in virology,* vol. 2011, p. 535206, 2011 (Epub 2011 Nov 2011.
[51] M. J. Rust, M. Lakadamyali, F. Zhang, and X. W. Zhuang, "Assembly of endocytic machinery around individual influenza viruses during viral entry," *Nature Structural & Molecular Biology,* vol. 11, pp. 567-573, Jun 2004.
[52] P. Verdijk, P. A. van Veelen, A. H. de Ru, P. J. Hensbergen, K. Mizuno, H. K. Koerten*, et al.*, "Morphological changes during dendritic cell maturation correlate with cofilin activation and translocation to the cell membrane," *European Journal of Immunology,* vol. 34, pp. 156-164, Jan 2004.
[53] R. M. Straubinger, D. Papahadjopoulos, and K. Hong, "Endocytosis and intracellular fate of liposomes using pyranine as a probe," *Biochemistry,* vol. 29, pp. 4929-4939, May 1990.
[54] D. Kirpotin, J. W. Park, K. Hong, S. Zalipsky, W. L. Li, P. Carter*, et al.*, "Sterically stabilized Anti-HER2 immunoliposomes: Design and targeting to human breast cancer cells in vitro," *Biochemistry,* vol. 36, pp. 66-75, Jan 1997.
[55] T. Okano, Y. H. Bae, H. Jacobs, and S. W. Kim, "Thermally on-off switching polymers for drug permeation and release," *Journal of Controlled Release,* vol. 11, pp. 255-265, Jan 1990.

APPENDIX A

PKH67 staining protocol

- Uniform suspension of well-dispersed single cells in tissue culture medium
- Tissue culture medium with serum (complete medium)
- Ca^{2+}, Mg^{2+}, and serum free medium or buffered salt solution (e.g., Dulbecco's PBS or Hank's BSS)
- Serum, albumin, or other system-compatible protein
- Polypropylene conical bottom centrifuge tubes (4–15 mL)
- Temperature-controlled centrifuge (up to 1,000×*g*)
- Instrument(s) for fluorescence analysis (fluorescence plate reader, fluorescence or confocal microscope, flow cytometer)
- Laminar flow hood
- Hemocytometer or cell counter
- Slides and coverslips

The following procedure uses a 2 mL final staining volume containing final concentrations of 2×10^{-6} M of PKH67 and 1×10^{7} cells/mL.

Perform all further steps at ambient temperature (20–25 °C)

1. Place a suspension containing 2×10^{7} single cells in a conical bottom polypropylene tube and wash once using medium without serum.

2. Centrifuge the cells (400×*g*) for 5 minutes into a loose pellet.

3. After centrifuging cells, carefully aspirate the supernatant, being careful not to remove any cells but leaving no more than 25 µL of supernatant.

4. Prepare a 2× Cell Suspension by adding 1 mL of Diluent C (Catalog Number CGLDIL) to the cell pellet and resuspend with gentle pipetting to insure complete dispersion. **Do not vortex and do not let cells stand in Diluent C for long periods of time**.

5. **Immediately prior to staining**, prepare a 2× Dye Solution (4×10^{-6} M) in Diluent C by adding 4 µL of the PKH67 ethanolic dye solution (Catalog Number P7333) to 1 mL of Diluent C in a polypropylene centrifuge tube and mix well to disperse.

6. **Rapidly add** the 1 mL of 2× Cell Suspension (step 4) to 1 mL of 2× Dye Solution (step 5) and **immediately mix** the sample by pipetting. Final concentrations after mixing the indicated volumes will be 1×10^{7} cells/mL and 2×10^{-6} M PKH67.

7. Incubate the cell/dye suspension from step 6 for 1–5 minutes with periodic mixing. Because staining is so rapid, longer times provide no advantage.

8. Stop the staining by adding an equal volume (2 mL) of serum or other suitable protein solution (e.g., 1% BSA) and incubate for 1 minute to allow binding of excess dye.

9. Centrifuge the cells at 400×g for 10 minutes at 20-25 °C and carefully remove the supernatant, being sure not to remove cells. Resuspend cell pellet in 10 mL of complete medium, transfer to a fresh sterile conical poly-propylene tube, centrifuge at 400×g for 5 minutes at 20-25 °C, and wash the cell pellet 2 more times with 10 mL of complete medium to ensure removal of unbound dye.

10. After the final wash, resuspend the cell pellet in 10 mL of complete medium for assessment of cell recovery, cell viability and fluorescence intensity. Centrifuge and resuspend to desired final concentration of viable cells.

Chalmers University of Technology
SE-412 96 Gothenburg, Sweden
Telephone: + 46 (0)31-772 1000